CONTROL OF CELL FATE DECISIONS OF EMBRYONIC STEM CELLS BY MECHANICAL FORCES

BY

FARHAN HYDER CHOWDHURY

DISSERTATION

Submitted in partial fulfillment of the requirements
for the degree of Doctor of Philosophy in Mechanical Engineering
in the Graduate College of the
University of Illinois at Urbana-Champaign, 2011

Urbana, Illinois

Doctoral Committee:

Professor Ning Wang, Chair
Associate Professor Min-Feng Yu
Assistant Professor Tetsuya Tanaka
Assistant Professor Fei Wang

ABSTRACT

Mounting evidences implicate mechanical properties of the substrates, upon which the cells adhere, to influence critical biological functions including cell fate decisions in mesenchymal stem cells. However, how embryonic stem cells respond to forces or underlying substrates is not clear at this time. The work presented here examines how mouse embryonic stem cells (mESCs) respond to externally applied forces and underlying substrates. We examined if mESCs can be directed to differentiate by external local forces through integrin mediated pathway. Surprisingly, we found that cyclic loading of the same stress amplitude can induce cell spreading in mouse embryonic stem cells but not in $\sim$10 times stiffer differentiated cells. The stress induced spreading response was dictated by cell softness, suggesting that it is the intracellular deformation of the cytoskeleton that dictates cell spreading response. A local stress via focal adhesions alone can induce embryonic stem cells to differentiate, in the absence of soluble differentiation factors.

Now that we see that mESCs can be directed to differentiation solely by external mechanical forces, we next examined if mESCs can be kept in their pluripotent state by culturing them on soft substrates. We found that soft substrates that match the intrinsic stiffness of the cell can maintain populations of mESC culture homogeneously in an undifferentiated state. The underlying biophysical mechanism is to match matrix substrate stiffness to that of the mESCs which in turn generates low cell-matrix tractions and low colony stiffness correlating well with compact and round colony morphology, expressed high levels of OCT3/4, NANOG, and the Alkaline Phosphatase activity, even in the absence of Leukemia Inhibitory Factor (LIF). The mESCs on the soft substrates formed more efficient embryoid bodies and teratomas than those on rigid substrates. Collectively, these results strongly suggest that mechanics is indispensable in physiological functions of embryonic stem cells.

To my beloved daughter, Zoya.

ACKNOWLEDGMENTS

I would like to thank my parents, siblings, in-laws, and friends for their encouragement and best wishes. I especially thank my wife Sabrina for her continued support over the years. She stood by me through the good times and bad. My daughter Zoya has always been and will continue to be my endless source of inspiration. I also thank Zoya for proofreading my dissertation! I would like to express my deepest gratitude to my advisor Professor Ning Wang for his guidance and support. He was always accessible and eager to rescue me when I was getting lost. His thoughtful insights and constructive feedback made a huge difference in my academic life, in writing several original research manuscripts, and this dissertation. In the same vein, I also would like to thank my committee members Drs. Fei Wang, Min-Feng Yu and Tetsuya Tanaka for their time and valuable comments and suggestions which made this dissertation more complete. I especially would to take this opportunity to express my gratitude to Dr. Tanaka for being so helpful and accommodating. I learned a lot from him.

I also would like to thank all Wang lab members, both past and present, for making the lab a congenial workplace. I especially thank Sungsoo and Olivier for giving me basic research training in cell mechanics and biology. I thank Poh for his help and feedback. I also thank Neha for technical assistance. I enjoyed discussions with Michael, Bernard, Kevin, Russell, Poh, Arash, Yuhei, and Youhua. Our everyday discussions related or unrelated to research was possible as all Wang Lab members shared the same room as their offices. Thanks to Professor Wang for keeping it that way. I also take this opportunity to thank both Fei and Tanaka lab members- Dong, Myung, Yanzhen, Paige, and Tamaki. I would like to thank my friend Hasib for his time and effort to help me format this dissertation using LaTeX . The last but not least, I acknowledge NIH and University of Illinois for supporting me during the past five years.

TABLE OF CONTENTS

LIST OF FIGURES

LIST OF ABBREVIATIONS

ESCs	Embyonic Stem Cells
mESCs	Mouse Embyonic Stem Cells
hESCs	Human Embyonic Stem Cells
MSCs	Mesenchymal Stem Cells
iPSCs	Induced Pluripotent Stem Cells
EB	Embryoid Body
LIF	Leukemia Inhibitory Factor
bFGF	Basic Fibroblast Growth Factor
TGF-β	Transforming Growth Factor Beta
E-cadherin	Epithelial cadherin
NMMIIA	Nonmuscle Myosin IIA
Pa	Pascal
kPa	Kilo Pascal
MPa	Mega Pascal
GPa	Giga Pascal

CHAPTER 1

INTRODUCTION

1.1 Soluble factors influence pluripotency and differentiation

Stem cells isolated from the embryonic stages of development can self renew in culture and holds a promising future for therapeutic applications. However adapting them to *in vitro* culture system encounters an unrelenting challenge of keeping them undifferentiated and directing their differentiation ever since the first isolation of mouse embryonic stem cells (mESCs) in 1981 [1]. Fairly a large amount of studies have been dedicated to understand how soluble factors like cytokines, hormones, growth factors, and animal sera can influence these cell types in terms of self renewal or cell-lineage specification [2-7]. Maintenance of mESCs was originally accomplished by using feeder layers or exogenous supply of soluble factor called leukemia inhibitory factor (LIF) together with serum or other soluble growth factors called bone morphogenic proteins which acts through the LIFR/gp130 complex to maintain pluripotency [3, 8]. Recently, the ground state of self renewal and pluripotency for embryonic stem cells has been described that eliminate the need for exogenous chemical stimuli like LIF for maintaining pluripotency simply by suppression of differentiation-inducing signaling from mitogen-activated protein kinase and glycogen synthase kinase (two inhibitors: 2i conditions) [9]. Interestingly however, maximal self-renewal is achieved by the combinatorial use of LIF and 2i validating LIF/STAT3 signaling as an essential component of self-renewal in ESCs [10]. Similar to mESCs, soluble factors have been shown to regulate pluripotency genes necessary to support long-term self-renewal and undifferentiated proliferation of human embryonic stem cells (hESCs). These soluble factors like basic FGF (bFGF) [11, 12], TGF-β [13], and insulin-like growth factor 1 [14] stabilizes a network of transcription

factors including OCT3/4, SOX2, and NANOG. More recently, it has been shown that the signals from the soluble factors are incorporated by intracellular molecules, such as mammalian target of rapamycin (mTOR) [15], to suppress differentiation activities and promote proliferation and survival of hESCs.

Library of small molecules are also being constantly screened to identify potential soluble factors that direct cells into particular lineages. To name a few, soluble growth factors like bone morphogenic proteins [16] was shown to inhibit ectodermal lineage differentiation. Conversely, retinoic acid [17] was shown to promote ectodermal lineage differentiation. Recently it was reported that the synergistic affect of salvianolic acid B and vitamin C induces cardiac differentiation programs [18].

More proprietary chemicals, natural products, and endogenous factors are screened and reported for the self-renewal or cell-lineage specification of embryonic stem cells or induced pluripotent stem cells (iPSCs). The use of small molecules have been successfully utilized in replacing some of the transgenic factors of Yamanaka cocktail (OCT3/4, SOX2, KLF4, C-MYC). For example, Melton et al. [19] reported that a small molecule valproic acid successfully increased the efficiencies of reprogramming with all four factors or replaced KLF4 and C-MYC altogether. In a similar fashion Eggan et al. [20] demonstrated that Repsox, a small-molecule inhibitor of TGF- signaling replaces SOX2 in the reprogramming process.

1.2 Does mechanics matter in the life of stem cells?

The conventional wisdom suggests that chemical signaling alone drive cell physiology. This current dogma was reshaped during the last decade from the convergence of studies involving engineers, physicists, and biologists. Consequently, in addition to soluble factors, the importance of physical microenvironment and mechanical stimuli became increasingly accepted as potent regulators of self-renewal or differentiation in both embryonic and adult stem cells [21-29]. These overwhelming evidences suggest that stem cells respond to different forms of mechanical cues like externally applied forces; multiaxial strains; passive microenvironment properties like change in substrate stiffness, geometric restrictions, and topography which ultimately regulate

cellular form and function. These results strongly suggest that mechanics is indispensable in stem cell physiology. Nevertheless, the mechanisms have not been fully understood yet. This is no trivial issue and remains a current challenge in the field. Unlike chemical signaling, which has been well studied and characterized, very little is known about mechanical signaling cascades. Recent findings show that downstream of the initial activation site on the cell surface, mechanical signaling is very much different from a growth factor induced signaling [30, 31]. Future studies may enable us to dissect out the essential pathways of mechanical signaling.

1.2.1 Mechanical factors and Mesenchymal stem cells (MSCs)

Mechanical and physical factors have been shown to regulate gene expression and fate determination of adult stem cells. Mechanical strains have been shown to control MSC gene expression as reported by Kurpinski et al [23]. Here they used a micropattened strip to align the MSCs along the direction of the uniaxial strain. Following the loading of strain the expression of a smooth muscle cell marker, calponin 1, was increased while cartilage matrix marker expression was decreased. However, when the strain was loaded in the perpendicular direction to the aligned cells, the changes in gene expression were diminished. These results strongly suggest that mechanical strain alone has a significant impact on MSC gene expression. MacBeath et al. [21] reported that changes in cell shape could regulate MSCs lineage determination. MSCs when allowed to spread on small micropatterned islands tend to differentiate preferentially into adipocytes while those allowed to spread on larger micropatterned islands differentiate into osteoblasts. Engler et al. [22] led the way to show the effect of substrate stiffness on the fate of MSCs. MSCs plated on soft (0.1-1 kPa) substrates (mimicking brain) differentiated preferentially into neurons, while those plated on intermediate (8-17 kPa) and rigid (25-40 kPa) substrates with stiffness similar to muscle and bone tissue underwent myogenic and osteogenic differentiation respectively. More recently, matrix stiffness alone was shown to maintain stemness of in muscle stem cells. Gilbert et al. [28] showed that muscle stem cells (MuSCs) when cultured on substrates that mimics the elasticity of muscle (12 kPa) greatly retained their regenerative potential.

1.2.2 Mechanical forces and ESCs

Although MSCs and other adult stem cell population hold a promising future in biomedical research and cell based therapies, they are downstream in cell-lineage specifications in comparison to ESCs. Additionally, ESCs offer an excellent *in vitro* tool to study development. Importantly, the effect of the mechanical forces and physical environment on ESCs has not been well investigated. We speculate mechanical perturbations are very much relevant in development as cells are exposed to both chemical and mechanical cues during gastrulation and during this crucial dynamic cellular rearrangement process they generate and experience tension, compression and shear forces [32]. Understanding the fundamental processes by which ESCs respond to mechanical forces is a key to understanding the mechanisms of development and lineage determination. Therefore, we focus on truly pluripotent ESCs to investigate how these cells would respond to physical and mechanical cues.

1.3 Topics covered in this dissertation

In chapter 2, we investigated the mechanosensitivity of ESCs by applying small amount of mechanical forces. Surprisingly, we found that ESCs are very sensitive to small mechanical forces. They start to spread in response to the applied forces and eventually differentiate. We also reveal the underlying mechanism for this behavior. This is exclusively due their intrinsic softness compared to other differentiated cells types. Consequently, for a given applied stress level, the resulting strain reaches a much higher value in ESCs than in other differentiated cell types. This resulting strain when reaches a certain strain threshold, the ESCs start to spread and eventually differentiate. The work presented in this chapter shows that ESCs can be differentiated into other cell types solely based on external mechanical forces.

The work presented in chapter 3 originates during the study carried out in chapter 2. Earlier we found that ESCs has an optimal baseline spreading on 0.6 kPa substrates which coincidentally happened to be their own intrinsic stiffness [33]. This is consistent to the fact that cell-substrate stiffness matching is crucial for normal cell functions [34]. This led to the investigation, addressing a long-standing problem in the field of stem cell biology, whether we can keep ESCs in an undifferentiated state of growth by manip-

ulating their local microenvironment. ESCs are adapted to *in vitro* culture condition by plating them on rigid plastic dishes which is ∼million times stiffer (in the order of GPa range, [28]) than their inherent stiffness. Consequently, the ESCs respond to the substrate stiffness by fluctuating expression of pluripotent and differentiated genes and the culture results in a heterogeneous cell population. This also hinders the induction of differentiation processes as precursor materials (ESCs) are non-homogeneous. Therefore, we hypothesized that culturing them on a substrate with similar stiffness as their intrinsic stiffness would be the key to this problem. Importantly, we showed the mechanism by which our novel method can keep these ESCs in an unlimited self-renewal state. This is solely due to the downregulation of cell-matrix traction generated by these cells. When we started elevate cell-matrix tractions, the ESCs began to lose self-renewal and pluripotency and started to differentiate.

In chapter 4, conclusions and future directions are discussed.

1.4 References

[1] Evans, M.J. and M.H. Kaufman, "Establishment in culture of pluripotential cells from mouse embryos". *Nature* 292(5819), pp.154-156, 1981.

[2] Niwa, H., T. Burdon, I. Chambers, and A. Smith, "Self-renewal of pluripotent embryonic stem cells is mediated via activation of STAT3". *Genes & Development* 12(13), pp.2048-2060, 1998.

[3] Yoshida, K. et al., "Maintenance of the pluripotential phenotype of embryonic stem cells through direct activation of gp130 signalling pathways". *Mechanisms of Development* 45(2), pp.163-171, 1994.

[4] Ying, Q.L., J. Nichols, I. Chambers, and A. Smith, "BMP induction of Id proteins suppresses differentiation and sustains embryonic stem cell self-renewal in collaboration with STAT3". *Cell* 115(3), pp.281-292, 2003.

[5] Sato, N., L. Meijer, L. Skaltsounis, P. Greengard, and A.H. Brivanlou, "Maintenance of pluripotency in human and mouse embryonic stem

cells through activation of Wnt signaling by a pharmacological GSK-3-specific inhibitor". *Nature Medicine* 10(1), pp.55-63, 2004.

[6] Rathjen, J. et al., "Formation of a primitive ectoderm like cell population, EPL cells, from ES cells in response to biologically derived factors". *J. Cell Sci.* 112(5), pp.601-612, 1999.

[7] Kunath, T. et al., "FGF stimulation of the Erk1/2 signalling cascade triggers transition of pluripotent embryonic stem cells from self-renewal to lineage commitment". *Development* 134(16), pp.2895-2902, 2007.

[8] Burdon, T., I. Chambers, C. Stracey, H. Niwa, and A. Smith, "Signaling mechanisms regulating self-renewal and differentiation of pluripotent embryonic stem cells". *Cells Tissues Organs* 165, pp.131-143, 1999.

[9] Ying, Q.L. et al., "The ground state of embryonic stem cell self-renewal". *Nature* 453, pp.519-523, 2008.

[10] Casanova, E.A. et al., "Pramel7 Mediates LIF/STAT3 Dependent Self-Renewal in Embryonic Stem Cells". *Stem Cells* 29(3), pp.474-85, 2011.

[11] Thomson, J.A. et al., "Embryonic stem cell lines derived from human blastocysts". *Science* 282(5391), pp.1145-1147, 1998.

[12] Levenstein, M.E. et al., "Basic fibroblast growth factor support of human embryonic stem cell self-renewal". *Stem Cells* 24(3), pp.568-574, 2006.

[13] Xu, R.H. et al., NANOG is a direct target of TGFbeta/activin-mediated SMAD signaling in human ESCs. *Cell Stem Cell* 3(2), pp.196-206, 2008.

[14] Bendall, S.C. et al., "IGF and FGF cooperatively establish the regulatory stem cell niche of pluripotent human cells in vitro". *Nature* 448(7157), pp.1015-1021, 2007.

[15] Zhou, J.P. et al., "mTOR supports longterm self-renewal and suppresses mesoderm and endoderm activities of human embryonic stem cells". *Proc. Natl. Acad. Sci. USA* 106(19), pp.7840-7845, 2009.

[16] Finley, M.F., S. Devata, and J.E. Huettner, "BMP-4 inhibits neural differentiation of murine embryonic stem cells". *Journal of Neurobiology* 40(3), pp.271-287, 1999.

[17] Fraichard, A. et al., "In vitro differentiation of embryonic stem cells into glial cells and functional neurons". *Journal of Cell Science* 108(10), pp.3181-3188, 1995.

[18] Chan, S.S. et al., "Salvianolic acid B-vitamin C synergy in cardiac differentiation from embryonic stem cells". *Biochemical and Biophysical Research Communications* 387(4), pp.723-728, 2009.

[19] Huangfu, D. et al., "Induction of pluripotent stem cells from primary human fibroblasts with only Oct4 and Sox2". *Nature Biotechnology* 26(11), pp.1269-1275, 2008.

[20] Ichida, J.K. et al., "A small-molecule inhibitor of tgf-Beta signaling replaces sox2 in reprogramming by inducing nanog". *Cell Stem Cell.* 5(5), pp.491-503, 2009.

[21] McBeath, R., D.M. Pirone, C.M. Nelson, K. Bhadriraju, and C.S. Chen, "Cell shape, cytoskeletal tension, and RhoA regulate stem cell lineage commitment". *Developmental Cell* 6(4), pp.483-495, 2004.

[22] Engler, A.J., S. Sen, H.L. Sweeney, and D.E. Discher, "Matrix elasticity directs stem cell lineage specification". *Cell* 126(4), pp.677-689, 2006.

[23] Kurpinski, K., J. Chu, C. Hashi, and S. Li, "Anisotropic mechanosensing by mesenchymal stem cells". *Proc. Natl. Acad. Sci. USA* 103(44), pp.16095-16100, 2006.

[24] Dalby, M.J. et al., "The control of human mesenchymal cell differentiation using nanoscale symmetry and disorder". *Nature Materials* 6(12), pp.997-1003, 2007.

[25] Adamo, L. et al., "Biomechanical forces promote embryonic haematopoiesis". *Nature* 459(7250), pp.1131-1135, 2009.

[26] Chowdhury, F. et al. "Material properties of the cell dictate stress-induced spreading and differentiation in embryonic stem cells". *Nat. Mater.* 9(1), pp.82-88, 2010.

[27] Chowdhury, F. et al. "Soft substrates promote homogeneous self-renewal of embryonic stem cells via downregulating cell-Matrix tractions". *PLoS ONE* 5, pp.e15655, 2010.

[28] Gilbert, P.M. et al. "Substrate elasticity regulates skeletal muscle stem cell self-renewal in culture". *Science* 329(5995), pp.1078-1081, 2010.

[29] Li, D. et al. "Role of mechanical factors in fate decisions of stem cells". *Regenerative Medicine* 6(2), pp.229-240, 2011.

[30] Na, S. et al. "Rapid signal transduction in living cells is a unique feature of mechanotransduction". *Proc. Natl. Acad. Sci. USA* 105(18), pp.6626-6631, 2008.

[31] Poh, Y.C. et al. "Rapid activation of Rac GTPase in living cells by force is independent of Src". *PLoS ONE* 4(11), pp.e7886, 2009.

[32] Keller, R., L.A. Davidson, and D.R. Shook, "How we are shaped: the biomechanics of gastrulation". *Differentiation* 71(3), pp.171-205, 2003.

[33] Chowdhury, F. et al., "Is cell rheology governed by nonequilibrium-to-equilibrium transition of noncovalent bonds?". *Biophys. J.* 95(12), pp.5719-5727, 2008.

[34] Engler, A.J. et al., "Myotubes differentiate optimally on substrates with tissue-like stiffness: Pathological implications for soft or stiff microenvironments". *Journal of Cell Biology* 166(6), pp.877-887, 2004.

CHAPTER 2

MECHANICAL FORCE INDUCED SPREADING AND DIFFERENTIATION OF EMBRYONIC STEM CELLS

Adapted from Chowdhury et al. (2008) Biophysical Journal 95: 5719- 5727 and Chowdhury et al. (2010) Nature Materials 9: 82- 88

2.1 Abstract

Increasing evidences suggest that physical microenvironments and mechanical stresses, in addition to soluble factors, help direct mesenchymal stem cell fate. However, biological responses to a local force in ESCs remain unclear. Here we show that a local cyclic stress via focal adhesions induces spreading in mouse ES (mES) cells but not in mES cell-differentiated (ESD) cells that were 10-fold stiffer. This response was solely dictated by the intrinsic cell material property (cell softness), suggesting that reaching a threshold cellular strain is the key setpoint for triggering spreading responses. Cell-matrix traction quantification, pharmacological, and shRNA intervention indicated that myosin II contractility, F-actin, Src, or Cdc42 were essential in the spreading response. Following the application of the stress induced spreading; expression of OCT3/4 gene was found to be downregulated in these mES cells. These findings strongly demonstrate that cell softness dictates cellular sensitivity to force, implicating local small forces to play far more important roles in early developments of soft embryos than previously anticipated.

Key words: cell rheology, mechanotransduction, prestress, gene expression, strain

2.2 Introduction

Embryonic stem cells are one of the major focuses in biology because of their pluripotency and potential therapeutic applications [1-3]. Although it

is known that soluble factors are critical in stem cell differentiation [4, 5], recent evidence shows that the physical microenvironment of the cells (e.g., shape constraint or substrate stiffness) helps direct the fate of mesenchymal stem cells [6, 7]. These cells, however, are downstream in cell lineage specifications, and have limited self-renewal and differentiation capacities in comparison to ES cells. We focus on pluripotent ES cells since little is known about how these cells respond to mechanical forces. Understanding the fundamental processes by which ES cells respond to force is crucial in elucidating mechanisms of lineage determination and development as these cells are derived from the inner cell mass of blastocysts prior to gastrulation that initiates dynamic cellular rearrangements. It is known that living cells alter their shapes and functions in respond to mechanical forces. For example, unidirectional laminar shear flow stresses over a whole endothelial cell facilitate cell spreading and elongation in the direction of the flow [8]. Uniaxial stretching of a vascular smooth muscle cell elongates the cell in the direction of stretching [9]. Cyclic uniaxial stretching of whole mesenchymal stem cells increases cell proliferation and expression of smooth muscle cell markers [10]. Recently, it is reported that fluid shear stress over whole hematopoietic progenitor cells promotes embryonic hematopoiesis [11]. However, whether and how ES cells respond to a localized mechanical stress remain elusive. During the last decade or so, the importance of substrate rigidity in cell functions is becoming increasingly clear [7, 12-14]. The physical and mechanical cues of the extracellular matrix are transduced into intracellular rheological and biochemical changes via unknown mechanisms, but likely via conformational changes or unfolding of focal adhesion-based proteins [15] and other proteins. On the other hand, several researchers have proposed that intracellular rheological properties are critical in understanding cellular behaviors [16-18]. Therefore, it is suggested that intrinsic intracellular material mechanical properties govern cellular behaviors and functions. However, no experimental data are available to unequivocally show that intrinsic intracellular rheological properties of living cells are fundamentally important in cellular biological responses to force and in biological functions, despite recent discoveries at the molecular level on the unfolding of focal adhesion protein talin in vitro by force [15], on integrin activation by force in living endothelial cells [19], and on unfolding of spectrin in red blood cells by shear flow stress [20]. This is not a trivial issue. Since in general any individual

structural protein under stress is physically connected with the rest of the cytoskeleton network, the overall cells or cytoskeletons deformability should dictate how much this protein can be deformed as all forces must be balanced. In this study, we demonstrate that adherent mES cells are softer and much more sensitive to a local cyclic stress than their differentiated counterparts. We show that the material property of the cell, the cell softness, dictates the stress-induced spreading response. We reveal the underlying signaling pathways in stress-induced spreading in mES cells. OCT3/4 (Pou5f1) expression in mES cells [21] gradually disappears in response to the stress. Our results suggest that a local, small, cyclic stress plays a critical role in inducing strong biological responses in soft mES cells that originate from inner cell mass and in shaping embryogenesis during development.

2.3 Results

2.3.1 Baseline cell spreading of mES cells is optimum on 0.6 kPa substrates

First we measured the projected areas of mES cells and differentiated cells (derived from these mES cells) on different substrate stiffness overnight. As expected from a published report [22], the mES cell-differentiated (ESD) cells increased their projected areas with increasing substrate stiffness (Fig. 2.1). In contrast, mES cell projected areas were maximal at a substrate stiffness of 0.6 kPa, similar to the intrinsic elastic stiffness of these mES cells (Fig. 2.2). These results are consistent with a previous report that cell-substrate stiffness matching is crucial for normal cell functions [23].

2.3.2 mES cells initiates spreading in response to external stress

Next we explored whether these soft mES cells could respond to a localized external stress. After a mES cell was plated on the substrate of 0.6 kPa overnight, we attached a 4-μm RGD-coated magnetic bead on the apical surface of the cell and applied a small, oscillatory stress (17.5 Pa at 0.3 Hz) continuously (Fig. 2.3a). Surprisingly, this small local cyclic stress

induced time-dependent increases in the spreading of the mES cell. The stress-induced spreading occurred as early as ∼30 s after the onset of stress application (Fig. 2.3a). While it is expected that unidirectional stretching or stressing of a whole cell would elongate the cell in the direction of the stretching or the stress [8,9], it is not clear whether a small localized oscillatory stress of zero mean magnitude could induce cell protrusion and spreading in many different directions. mES cells on other magnitudes of substrate stiffness also spread in response to the applied stress but the extent of spreading was less, suggesting that the cell-substrate stiffness matching potentiates the optimal spreading response in mES cells to external stress. To quantify changes in cell area, we measured velocity profiles of the cell periphery using an established method [24]. The mES cell increased normal membrane protrusion velocity and spreading area as a function of stress application time (Fig. 2.3b-d). In sharp contrast, the stiff ESD cell on the same substrate stiffness did not exhibit any changes in normal velocity or cell projected area in response to the same amplitude of the cyclic stress (Fig. 2.3e-h). The lack of stress-induced ESD cell spreading is not due to the limitation of the spreading capacity of these cells, since they continue to spread on stiffer substrates (Fig. 2.1), likely to be driven by much greater myosin-II-dependent endogenous forces. The ESD cells on much stiffer substrates failed to spread in response to the external stress. The summarized data show that mES cells are much more sensitive to a localized cyclic stress than their differentiated counterpart ESD cells (Fig. 2.4a). The threshold amplitude of stress for mES cell spreading is between 3.5-17.5 Pa (Fig. 2.4a) and the optimal frequency for spreading is ∼0.3-1 Hz (Fig. 2.5), consistent with the published report that the optimal loading frequency for cytoskeletal deformation is ∼1 Hz [25]. Results from stiff human airway smooth muscle (ASM) cells (a well-established differentiated tissue cell type), plated on the same substrate (stiffness) that was coated with the same immobilized amount of collagen-1, showed that they did not spread to the same stress, similar to stiff ESD cells (Fig. 2.4a), suggesting that our findings that inversely correlating cell stiffness with spreading responsiveness can be generalized to other cell types.

2.3.3 Cell Softness dictates response to stress

To explore the underlying biophysical mechanism of stress-induced spreading in mES cells, we compared the softness of mES cells with that of ESD cells. Softness is defined as the ratio of strain to stress and is the inverse of stiffness. Softness of mES cells was ∼10 times higher than that of ESD cells on the same substrate (Fig. 2.4b). Since the applied stress was the same for both cell types, this result suggests that the soft mES cells were more responsive because of greater deformation or strains in these mES cells than in ESD cells. To further test this idea, we plated the ESD cells or the ASM cells on sparsely coated matrix proteins (1 ng/ml collagen-1 on rigid glass overnight) to limit their projected areas and to increase their softness. As predicted, these soft round intact ESD cells and ASM cells also started to spread in response the cyclic localized stress (Fig. 2.4 a, b). The greater the cell softness, the stronger the spreading response (i.e., the more increases in cell area in response to stress) (Fig. 2.4b). Furthermore, the relative softness of mES cells, round ESD cells, and ESD cells correlated inversely with respective densities of F-actin (Fig. 2.6), consistent with the established evidence that F-actin is a major determinant in cell stiffness [26].

2.3.4 Cell softness but not smaller projected area dictates stress induced spreading

An alternative interpretation to our data is that the smaller the projected cell area, the stronger the spreading response to the externally applied stress. This interpretation is based on the fact that the baseline projected areas of differentiated cells are larger than those of the mES cells on the same substrate (Fig. 2.2). Thus it is possible that the biochemical responses to stress in these differentiated cells (such as Ca^{2+} influx) might have been similar to those in undifferentiated mES cells, but these biochemical signals were just not potent enough to cause further spreading. To determine whether it is the cell softness or the cell baseline projected area that controls the spreading or protrusion sensitivity to stress, we plated ESD cells or ASM cells on micropatterned adhesive islands (25-μm diameter circles) on the 0.6 kPa substrate coated with high density of collagen-1 [27]. Each ESD cell or each ASM cell on each island had a similar projected area as the mES cell on

the 0.6 kPa substrate but was ∼8 times stiffer. The ESD cell and the ASM cell failed to extend any protrusions in response to the same applied stress, as the soft mES cell did (Fig. 2.4c). These data indicate that it is the cell softness, not the projected area, that controls the protrusion and spreading responsiveness to stress. Taken together, these data suggest that the underlying biophysical mechanism for stress-triggered spreading is the deformation of the cytoskeleton and its associated proteins, providing a biological consequence and a functional significance to the recent findings on stress-induced conformational changes and/or unfolding of signaling molecules [28] and focal adhesion structural proteins [15].

2.3.5 Stress induced spreading coincides with increase intraction and accumulation of pMLC

To further explore the underlying mechanical and biochemical mechanisms of stress-induced spreading in mES cells, we quantified changes in tractional stresses. Tractions at the cell periphery increased within the first few minutes of stress application (Fig. 2.7b), which coincided temporally with the increases in cell areas (Fig. 2.7a). The ∼50% elevation in tractions at the cell periphery (Fig. 2.7c) was preceded by ∼40% increases in phosphorylated myosin light chains at the cell periphery by 30 s (Fig. 2.7e), from the diffusive distribution pattern throughout the cytoplasm prior to the stress application (Fig. 2.7d), suggesting that myosin II-dependent traction generation at the cell periphery is essential in stress-induced spreading in mES cells.

2.3.6 Myosin II, Src, cdc42, F-actin but not rac is important in stress induced spreading

Consistent with the aforementioned interpretation, pretreatment of the mES cells with myosin II ATPase inhibitor blebbistatin (50 μM for 30 min) or with myosin light chain kinase inhibitor ML-7 (25 μM for 20 min) completely prevented stress-induced ES spreading (Fig. 2.8a; Fig. 2.9). Furthermore, pretreatment with Rho-associated kinase (ROCK) inhibitor Y27632 (50 μM for 20 min) also prevented spreading of mES cells (Fig. 2.8a; Fig. 2.9), suggesting that ROCK is also critical in this process. Importantly, pretreatment

with PP1 (10 μM for 1hr), a specific Src tyrosine phosphorylation inhibitor, blocked stress-induced ES cell spreading (Fig. 2.8a; Fig. 2.9). This result suggests that Src is critical in the initiation of stress-induced spreading, consistent with a published report on the role of Src in the spontaneous early spreading of adherent cells [29]. Interestingly, pretreatment with NSC23766 (100 μM for 1hr), a specific inhibitor of Rac [30,31], did not block stress-induced spreading, suggesting that Rac was not important in stress-induced spreading of mES cells (Fig. 2.8a, Fig. 2.9). The stress-induced cell spreading was specific to integrin-cytoskeleton pathways, since application of the same amplitude of stress via poly-L-lysine coated beads did not induce any changes in cell area in mES cells (Fig. 2.10), consistent with recent findings that rapid Src activation by stress only occurs via activated integrins [28] and that an applied stress via integrins induces additional activation of integrins and phosphorylation of focal adhesion kinase [19]. Stress-induced spreading in mES cells were completely prevented by pre-treatment with Latrunculin A (0.1 μg/ml for 30 min), consistent with the role of actin polymerization in cell protrusion and spreading. It should be noted that although these cytoskeletal drugs make the mES cells softer, they interfere with cytoskeletal dynamics and intracellular biochemical processes. Therefore these softer mES cells fail to spread in response to the applied stress, because cell spreading is a complex process that requires dynamic coordination of actin polymerization and myosin II [29]. It is known that Cdc42 mediates cell filopodia extension and cell spreading [32]. To determine the role of Cdc42 in stress-induced mES cell spreading, we infected the mES cells with small hairpin RNA (shRNA) for Cdc42 using lentiviruses. As shown in Fig. 2.8b and 2.8c (Fig. 2.11), Cdc42 knockdown correlated well with the abolishment of stress-induced spreading in these mES cells, consistent with published results in the role of Cdc42 in integrin-mediated spreading of differentiated cells [32]. Our finding that stress-induced spreading in these mES cells depends on Cdc42 but not on Rac is interesting since it is well known that integrin-mediated cell spreading depends on Rac in differentiated cells [32,33].

2.3.7 Stress-induced mES cell differentiation

To further determine the long term effects of a local cyclic stress in mES cell functions, we examined the expression of stably transfected GFP driven by OCT3/4 promoter in undifferentiated cells cultured in the presence of leukaemia inhibitory factor (+LIF) [34]. After a continuous application of a 17.5-Pa local stress at 0.3 Hz for only 60 min, OCT3/4 expression in these mES cells was downregulated by $\sim 35\%$ within 24 hrs, and by $\sim 50\%$ within 72 hrs, whereas control cells a few micrometers away in the same dish without stress continued to express OCT3/4 (Fig. 2.12, Fig. 2.13). Since loss of OCT3/4 expression in ES cells is one of the hallmarks for differentiation [35], our results suggest that a local cyclic stress via a focal adhesion might be sufficient to drive a mES cell to differentiate. If our findings could be extended to early animal embryos, it would provide a novel way of locally differentiating a single cell of early lineage while keeping nearby cells undifferentiated.

2.4 Discussion

Accumulating experimental evidence suggests that mechanical contractile forces play a role in development (reviewed in ref. [36]. However, inability to access animal embryonic cells during early development makes it difficult to determine how important mechanical forces are during early development of animals and how sensitive embryonic cells are to force. Cultured ES cells offer an excellent model for studying biological responses to force by inner cell mass cells. In a recent review, Discher et al. discuss the combined effects of growth factors, matrices, and mechanical forces in controlling stem cells [37]. The importance of substrate stiffness in stem cell differentiation is highlighted. However, the underlying mechanism remains unclear. Discher and colleagues have shown that substrate elasticity modulates intracellular rheology: stiffer matrices result in stiffer cells [7]. In contrast, we show here that intracellular softness can determine cellular biological sensitivity to force at fixed substrate rigidity. Our current work reveals a biophysical mechanism of ES cells in dictating how ES cells respond biologically to a local small force via integrins. Our findings that the softness of mES cells makes them very sensitive to a local cyclic stress of physiologic amplitudes suggest that

small local forces (either endogenously generated or from neighboring cells) might play far more important roles in early embryogenesis and development of animals than previously appreciated. Our result that the cytoplasm of mES cells is intrinsically soft is also in accord with a previous finding that the nucleus of human ES cells is intrinsically soft [38].

Currently it remains elusive what are the intracellular molecular strain sensor(s) in a live cell, although the extracellular domains of integrins have been shown to undergo force-dependent conformational change to enhance adhesion [19], possibly via the catch bond mechanism [39]. However, accumulating evidence points to the deformation of focal adhesion proteins and possibly other structural proteins as the molecular mechanism of strain sensing. For example, in vitro forcing experiments show that unfolding single talin rods activates vinculin binding [15]. It is likely that time-varying, strain-dependent conformational changes and/or unfolding of these protein molecules at focal adhesions [40] and at other distant sites [41] (e.g., inside the nucleus) are the primary molecular mechanisms of mechanochemical transduction and strain-activated feedback loops [42]. An important test of this hypothesis will be to extend the in vitro work of del Rio et al. [15] to a live cell using physiologically relevant magnitudes of time-varying stresses. In addition, we speculate that focal adhesion-based protein opening and/or tyrosine kinase/phosphatase activation not only depends on the modulus of this individual molecule, but also depends on the collective modulus (or its inverse, softness) of the surrounding molecules and nearby cytoskeletal networks. The reason is that force must be balanced everywhere; therefore, the local cell softness near a focal adhesion must be crucial in determining how much a single molecule, such as talin, and other proteins, can be deformed and thus activated.

It might not be a coincidence that an unfertilized egg has a stiffness of $\sim$10 Pa (43), an ES cell has a stiffness of $\sim$500 Pa (Fig. 2.2), a brain neural cell has a stiffness of $\sim$100-500 Pa [12], a typical differentiated tissue cell (e.g., a smooth muscle cell) has a stiffness of 1-5 kPa [44], a skeletal muscle cell has a stiffness of $\sim$12 kPa [23]. The respective softness of various types of cells might manifest their different physiological functions and sensitivities to force in a multi-cellular organism. An evolutionary advantage for an early lineage cell to become stiffer as the cell divides and differentiates into a more differentiated tissue cell might be to protect the organism from injuries by

force, since the ability to respond to touch and to resist mechanical stress is postulated to be one of the most primitive features of metazoans that had evolved millions of years ago. Matching cell material property with that of its substrate is known to be critical in forming striation in skeletal muscle cells [23] and optimizing cadiomyocyte beating [45], but stiffness matching may have broader implications. As proposed recently [46], nutrient-rich uncompacted soft ocean sediments ∼2 billion years ago provided a selective evolutionary pressure favoring those very earliest eukaryotes that were better able to perform mechanical functions of invasion, crawling and forage, which are optimized when material properties of the cell match those of their very soft paste-like microenvironment. We perhaps see here in the ES cell the echo of those early evolutionary events. It is established that stress can regulate gene expression, but those previous studies are generally performed by stretching or fluid flow shearing whole cell surfaces, followed by analyses of average biological responses from millions of cells. Hence, it is difficult to elucidate mechanisms of mechanosensing and mechanotransduction. To our knowledge, our current study reveals for the first time that a small cyclic stress over a focal adhesion can downregulate OCT3/4 gene expression in single mES cells, likely due to the soft material property of these cells. Future studies are needed to elucidate the specific mechanisms of stress-induced inhibition of OCT3/4 expression in these mES cells, to determine if these findings can be extended to human ES cells and induced pluripotent stem (iPS) cells, and to find out whether stress-induced signals inhibit known pluripotency-supporting pathways mediated by molecules such as mTOR [47]. It will also be interesting to determine what type of differentiated cells can be derived from these soft ES cells by what mode of mechanical perturbations.

2.5 Methods

2.5.1 Cell culture and differentiation assay

Cells were thawed and cultured as described previously [48]. In short, undifferentiated mouse embryonic stem (mES) cells (W4, 129/SvEv) were maintained in the standard culture condition in the presence of Leukaemia In-

hibitory Factor (LIF; Chemicon). mES cells at passage 11 were thawed onto a feeder layer of mitoticallyinactivated primary murine embryonic fibroblasts (mEF). mES cells were passaged onto culture dishes coated with 0.1% gelatin for several times in every 2 days to remove feeders. For the differentiation assay, trypsinized mES cells, at passage 15-16, were plated on gelatin-coated dishes at a low density of 100 cells/cm^2. Following day, the mES cells were fed with the medium without LIF and with 1 μM Retinoic Acid (all-trans, Sigma) (-LIF/+RA). The mES cells in these conditions were fed with fresh medium every day for 4-5 days before experiment. In -LIF/+RA culture condition mES cells became differentiated to a heterogeneous population of differentiated cells (ESD) cells which were cultured with the complete medium. Human airway smooth muscle (ASM) cells were isolated at autopsy within 8 hrs of death from tracheal muscle of lung transplant donors (approved by the University of Pennsylvania Committee on studies involving human beings) at University of Pennsylvania in Dr. Panettieris laboratory [49]. We used de-identified HASM cells supplied by Dr. Panettieri who obtained the tissue through NDRI (National Disease Research Interchange) in a manner that excludes all unique identifying information. All our procedures were approved by the Institutional Review Board of University of Illinois at Urbana-Champaign. The ASM cells were cultured following published protocols [28].

2.5.2 Quantification of membrane protrusion velocity profiles

Edge velocity profiles display the edge dynamics during cell spreading. This technique is described before in details [24]. We utilized their approach (CellMAP) where input was a high contrast time lapse sequence (5 sec interval) of a single cell and the outputs were the normal cell edge velocity as a function of space (over entire arclength) and time, mean normal velocity over time, and change in cell area.

2.5.3 Applying a local stress using magnetic twisting cytometry

Magnetic twisting cytometry (MTC) is a well established method for applying controlled and precise local mechanical stresses of physiologic magnitudes to a living cell [18, 26, 44, 48, 50]. Briefly, ferromagnetic microbeads (4 m in diameter) were coated with ligands to integrin receptors (a synthetic peptide containing the ArgGlyAsp (RGD) sequence) or with poly-l-lysine (Sigma), both at 50 μg/ml per mg bead. The RGD-coated beads were incubated for 10-15 min to adhere to the apical surface of the cells so that they become tightly bound to the F-actin cytoskeleton via focal adhesions. The beads were magnetized horizontally using a strong (1000 gauss (G)) and short (<0.1ms) magnetic impulse. A twisting field was applied by a sinusoidally varying perpendicular magnetic field resulting in translational bead displacement induced by bead rotation. The bead movement was quantified using an intensity weighted center of mass algorithm. An inverted Leica microscope was used. A black and white charge-coupled device camera (Hamamatsu, C4742-95-12ERG) was attached to the camera side port of the microscope. Image acquisition was phase-locked with the sinusoidal twisting field. In our study, the magnetic twisting field was varied at 0.03, 0.3, 1, or 3 Hz. The amplitude of the oscillating field was varied at 0, 10, or 50 G. The apparent applied stress defined as the ratio of the applied torque to six times the bead volume and equals the bead constant times the applied twisting field. The bead constant was calibrated in a viscosity standard and determined to be 0.35 Pa per G. Therefore, the applied stress was 0, 3.5, or 17.5 Pa corresponding to the above applied magnetic field respectively. In all our loading experiments, mES cells were plated in low serum medium (1%). However, we found that a local cyclic stress also induced cell spreading in mES cells in the absence of serum, although at longer times, the extent of spreading appeared to be somewhat less prominent in zero serum than in 1% serum (Fig. 2.15).

2.5.4 Cell softness quantification

Cell stiffness measurement technique is described before [18, 25, 26, 44, 48, 50]. The cell complex softness is defined as the ratio of strain to the applied stress (i.e., the applied specific torque) and thus is the inverse of the cell

complex stiffness. Cell softness (unit=kPa-1) is a useful parameter here because molecular motors (e.g., myosin II) are force (the independent variable) generators and because strain-dependent opening of proteins are likely to be important in changing protein activities and cell functions [15]. The method is described briefly as following. Acquired bead displacements in response to the applied stress were stored for further analysis using a custom-made Matlab program. Bead displacements were displayed on an image window where one could select individual beads for analysis. The beads whose displacement waves conformed to the input sinusoidal signals at the same frequency were selected. This was necessary to filter out spontaneous movements of the beads or microscope stage shifts. Beads with displacements less than 5 nm (detection resolution) and loosely bound beads were not selected for analysis. To increase the signal to noise ratio, the peak amplitude of the displacement d (nm) was averaged over 5 consecutive cycles. The complex stiffness is measured by applying an oscillatory magnetic field and measuring the resultant oscillatory bead motions using the relation G*=T/d. For each bead, the elastic stiffness G (the real part of G*) and the dissipative stiffness G (the imaginary part of G*) was calculated based on the phase lag. The measured stiffness has the units of torque per unit bead volume per unit bead displacement (Pa/nm), which is model-free. In our cells the bead was embedded ∼50% into the cell surface (Fig. 2.16), similar to those found in other cell types in a recent report [51]. If one uses a 50% bead-cell surface contact area and an established finite element model to convert stiffness (Pa/nm) to modulus (Pa) [52], then 1 Pa/nm stiffness is equivalent to 2.5 kPa modulus. Cell softness values were obtained by taking the inverse of the cell modulus values and have the unit of kPa^{-1}.

2.5.5 Cell area and traction measurements

Cell spreading area was measured by ImageJ (NIH) using active contours algorithm. Cell traction measurements have been described in details elsewhere [46]. Briefly, a displacement field was calculated by comparing a fluorescent submicron bead image at a particular time point during the experiment with a reference image captured at the end of the experiment by trypsinizing the cell from its underlying substrates. Knowing the substrate rigidity and

the displacement field, a traction field was computed by solving this inverse problem. Therefore, the generated traction maps were used for further quantification. Based on the gray scale traction field we took a one micron thick annular section at the cell boundary at different time points and measured the intensity. Mean intensity within the annular section, representing the tractional stress developed at the cell boundary, at time zero (before twisting of magnetic bead) was set to 1 arbitrary unit (A.U.). Traction profiles were plotted over time around the boundary.

2.5.6 Lentivirus production and mES cell infection

For shRNA-mediated knockdown of Cdc42, the pLKO.1-puro Vector (Sigma-Aldrich) was used. We used Viralpower Lentivirus Packaging System (Invitrogen) to package lentivirus for Cdc42 knockdown, following the manufacturers instructions. Briefly, HEK293T cells were purchased from American Type Culture Collection (ATCC) and were cultured according to ATCC recommendations. HEK293T cells were plated for 24 hrs before transfection. After reaching $70 - 80\%$ confluency, cells were transfected with target or non-target shRNA control plasmids using the Fugene 6 reagent (Roche). The medium was replaced after overnight incubation of cells, with the virus packaging medium containing DMEM, 30% FBS, 1 mM sodium pyruvate, 4mM glutamine. Supernatant containing the lentivirus was collected 48-72 h later. To infect mES cells, lentiviruses were mixed with mES cells culture medium, and the mixture was incubated with 0.25% Trypsin-EDTA digested mES cells for 12 h. 6 μg/ml Polybrene (Sigma) was used to improve the efficiency of infection. Virus-containing medium was changed with fresh culture medium. After 5 d, the cells were harvested for additional assay.

2.5.7 Western Blot

To quantify Cdc42, infected mES cells were lysed directly with 200 μl laemmli sample buffer (BIO-RAD). 20 μl of each sample were analyzed by Western Blotting. The blots were developed using SuperSignal West Pico Chemiluminescent Substrate (Pierce).

2.5.8 EGFP and DsRed expressions in mES cells driven by OCT3/4 and CAGGS promoter

A mouse ES cell line, namely OGR1, that expresses EGFP under the promoter of OCT3/4 (OCT3/4::EGFP) [53] was transfected with 0.5 μg of pCAGGSDsRedT3_T2A_Puro (T. S. Tanaka et al., unpublished results) with FuGene (Roche) according to the manufacturer. Then, OGR1 that expresses DsRed.T3 stably was selected by puromycin (2 μg/ml; Invitrogen). DsRed.T3 has no toxicity in mouse ES cells [54].

2.5.9 Stress-mediated differentiation

To investigate if local application of a local cyclic stress is capable of down-regulating OCT3/4 expression in the long term, we used OGR1 cell line that simultaneously expresses EGFP and DsRed driven by OCT3/4 and CAGGS respectively. mES cells were plated sparsely on 0.6 kPa substrates on top of grid dishes to track particular cells of interest over a long period. Ferromagnetic magnetic beads were attached to the apical surface of the cells via integrins and incubated for 15 min. A 17.5-Pa local stress at 0.3 Hz was applied for $\sim$1 hr, which increased mES cell spreading area by $\sim$65% (Fig. 2.17). EGFP and DsRed expressions driven by OCT3/4 and by CAGGS promoter respectively were monitored every few hours. Continued expression of DsRed, under the promoter CAGGS, indicates the cell to be in an active state of translation. Loss of EGFP expression indicates down-regulation of OCT3/4, one of the hallmarks for differentiation. The stressed cells were labeled as +stress, +LIF/-RA condition. The cells without beads (i.e., no stress) in the same dish were also monitored (-stress, +LIF/-RA). Other dishes were monitored and EGFP-OCT3/4 were quantified as negative (+LIF/-RA) or positive (LIF/+RA) controls. 1 M retinoic acid (RA) was used in the LIF/+RA condition. Students t-test was used for all statistical analyses.

2.5.10 Variation of polyacrylamide gel substrate stiffness

Polyacrylamide gels were made as described before [55, 56]. The elastic Youngs modulus of the polyacrylamide gels used in this study was 0.15 kPa

(0.04% bis-acrylamide, 3% polyacrylamide), 0.6 kPa (0.06% bis-acrylamide, 3% polyacrylamide), 3.5 kPa (0.1% bis-acrylamide, 5% polyacrylamide) and 8 kPa (0.3% bis-acrylamide, 5% polyacrylamide) [57, 58]. $0.2\mu m$ yellow-green fluorescent microspheres (Molecular Probe) were embedded onto the gels for traction measurements. In some experiments, prepared gels and rigid glass substrates were coated with type I collagen (100 μg/ml and 40 μg/ml respectively). In some experiments, rigid glass substrates were coated with low type I collagen concentration of 1 ng/ml to maintain the cell in a rounded shape. Micropatterned adhesive islands on soft polyacrylamide gels were produced following published methods [27].

2.5.11 Drugs, antibodies, and immunofluorescence staining

LatA, PDGF, Rhodamine-phalloidin, Hoechst 33342 were from Sigma. Blebbistatin was from Toronto Research Chemicals. PP1 and ML-7 were from Biomol. NSC23766 was from Tocris Bioscience. Y-27632 was from Calbiochem. Anti phospho-MLC antibodies (Thr18/ Ser19, IF 1:50) and Cdc42 antibodies (WB 1:1000) were from Cell Signaling Technology. Goat anti-GAPDH (HRP) polyclonal antibody (WB 1:10,000) from Genscript Corporation and secondary antibodies (IF 1:100 and 1:200, WB 1:10,000) were from Abcam. For immunofluorescence microscopy, cells were fixed with 4% paraformaldehyde and permeabilized with 0.5% Triton X-100. Cells were incubated with primary antibodies at 4°C overnight and secondary antibody labeling was performed at room temperature for 1 hr. The actin cytoskeleton was stained using 0.76 μM Rhodamine-phalloidin for 20 minutes. The DNA was counter-stained with 1-10 μg/ml Hoechst 33342 for 10 min and the coverslips were rinsed three times in cytoskeleton buffer solution and once in dH_2O before mounting. F-actin content was quantified along the lines shown using ImageJ.

2.6 References

[1] Daley, G.Q. and D.T. Scadden, "Prospects for stem cell-based therapy". *Cell* 132, pp.544-548, 2008.

[2] Dimos, J. T. et al., "Induced pluripotent stem cells generated from patients with ALS can be differentiated into motor neurons". *Science* 321, pp.1218-1221, 2008.

[3] Soldner, F. et al., "Parkinson's disease patient-derived induced pluripotent stem cells free of viral reprogramming factors". *Cell* 136, pp.964-977, 2009.

[4] Park, I.H. et al., "Reprogramming of human somatic cells to pluripotency with defined factors". *Nature* 451, pp.141-146, 2008.

[5] Egli, D., G. Birkhoff, and K. Eggan, "Mediators of reprogramming: transcription factors and transitions through mitosis". *Nat. Rev. Mol. Cell Biol.* 9, pp.505-516, 2008.

[6] McBeath, R., D.M. Pirone, C.M. Nelson, K. Bhadriraju, and C.S. Chen, "Cell shape, cytoskeletal tension, and RhoA regulate stem cell lineage commitment". *Dev. Cell* 6, pp.483-495, 2004.

[7] Engler, A.J., S. Sen, H.L. Sweeney, and D.E. Discher, "Matrix elasticity directs stem cell lineage specification". *Cell* 126, pp.677-689, 2006.

[8] Wu, C.C. et al., "Directional shear flow and Rho activation prevent the endothelial cell apoptosis induced by micropatterned anisotropic geometry". *Proc. Natl. Acad. Sci. U.S.A.* 104, pp.1254-1259, 2007.

[9] Katsumi, A. et al., "Effects of cell tension on the small GTPase Rac". *J. Cell Biol.* 158, pp.153-164, 2002.

[10] Kurpinski, K., J. Chu, C. Hashi, and S. Li, "Anisotropic mechanosensing by mesenchymal stem cells". *Proc. Natl. Acad. Sci. U.S.A.* 103, pp.16095-16100, 2006.

[11] Adamo, L. et al., Biomechanical forces promote embryonic haematopoiesis. *Nature* 459, pp.1131-1135, 2009.

[12] Discher, D.E., P. Janmey, and Y.L. Wang, "Tissue cells feel and respond to the stiffness of their substrate". *Science* 310, pp.1139-1143, 2005.

[13] Vogel, V. and M.P. Sheetz, Local force and geometry sensing regulate cell functions. *Nat Rev Mol Cell Biol.* 7, pp.265-275, 2006.

[14] Mammoto, A. et al., "A mechanosensitive transcriptional mechanism that controls angiogenesis". *Nature* 457, pp.1103-1108, 2009.

[15] del Rio, A. et al., "Stretching single talin rod molecules activates vinculin binding". *Science* 323, pp.638-641, 2009.

[16] Mizuno, D., C. Tardin, C.F. Schmidt, and F.C. Mackintosh, "Nonequilibrium mechanics of active cytoskeletal networks". *Science* 315, pp.370-373, 2007.

[17] Weitz, D.A. and P.A. Janmey, "The soft framework of the cellular machine". *Proc. Natl. Acad. Sci. USA* 105, pp.1105-1106, 2008.

[18] Trepat, X. et al., "Universal physical responses to stretch in the living cell". *Nature* 447, pp.592-595, 2007.

[19] Friedland, J.C., M.H. Lee, and D. Boettiger, "Mechanically activated integrin switch controls alpha5beta1 function". *Science* 323, pp.642-644, 2009.

[20] Johnson, C.P., H.Y. Tang, C. Carag, D.W. Speicher, and D.E. Discher, "Forced unfolding of proteins within cells". *Science* 317, pp.663-666, 2007.

[21] Scholer, H.R., S. Ruppert, N. Suzuki, K. Chowdhury, and P. Gruss, "New type of POU domain in germ line-specific protein Oct-4". *Nature* 344, pp.435-439, 1990.

[22] Solon, J., I. Levental, K. Sengupta, P.C. Georges, and P.A. Janmey, "Fibroblast adaptation and stiffness matching to soft elastic substrates". *Biophys. J.* 93, pp.4453-4461, 2007.

[23] Engler, A.J. et al., "Myotubes differentiate optimally on substrates with tissue-like stiffness: pathological implications for soft or stiff microenvironments". *J. Cell Biol.* 166, pp.877-887, 2004.

[24] Dubin-Thaler, B.J. et al., "Quantification of cell edge velocities and traction forces reveals distinct motility modules during cell spreading". *PLoS ONE* 3, pp.e3735, 2008.

[25] Hu, S. and N. Wang, "Control of stress propagation in the cytoplasm by prestress and loading frequency". *Mol. Cell Biomech.* 3, pp.49-60, 2006.

[26] Wang, N., J.P. Butler, and D.E. Ingber, "Mechanotransduction across the cell surface and through the cytoskeleton". *Science* 260, pp.1124-1127, 1993.

[27] Wang, N., E. Ostuni, G.M. Whitesides, and D.E. Ingber, "Micropatterning tractional forces in living cells". *Cell Motil Cytoskeleton* 52, pp.97-106, 2002.

[28] Na, S. et al., "Rapid signal transduction in living cells is a unique feature of mechanotransduction". *Proc. Natl. Acad. Sci. USA* 105, pp.6626-6631, 2008.

[29] Zhang, X. et al., "Talin depletion reveals independence of initial cell spreading from integrin activation and traction". *Nat. Cell Biol.* 10, pp.1062-1068, 2008.

[30] Gao, Y., J. B. Dickerson, F. Guo, J. Zheng, and Y. Zheng, Rational design and characterization of a Rac GTPase-specific small molecule inhibitor. *Proc. Natl. Acad. Sci. USA* 101, pp.7618-7623, 2004.

[31] Habib, A. et al., "Modulation of COX-2 expression by statins in human monocytic cells". *FASEB J.* 21, pp.1665-1674, 2007.

[32] Price, L.S., J. Leng, M.A. Schwartz, and G.M. Bokoch, "Activation of Rac and Cdc42 by integrins mediates cell spreading". *Mol. Biol. Cell* 9, pp.1863-1871, 1998.

[33] D'Souza-Schorey, C., B. Boettner, and L. Van Aelst, "Rac regulates integrin-mediated spreading and increased adhesion of T lymphocytes". *Mol. Cell Biol.* 18, pp.3936-3946, 1998.

[34] Smith, A.G. et al., "Inhibition of pluripotential embryonic stem cell differentiation by purified polypeptides". *Nature* 336, pp.688-690, 1988.

[35] Walker, E. et al., "Prediction and testing of novel transcriptional networks regulating embryonic stem cell self-renewal and commitment". *Cell Stem Cell* 1, pp.71-86, 2007.

[36] Wozniak, M.A. and C.S. Chen, "Mechanotransduction in development: a growing role for contractility". *Nat. Rev. Mol. Cell Biol.* 10, pp.34-43, 2009.

[37] Discher, D.E., D.J. Mooney, and P.W. Zandstra, "Growth factors, matrices, and forces combine and control stem cells". *Science* 324, pp.1673-1677, 2009.

[38] Pajerowski, J.D., K.N. Dahl, F.L. Zhong, P.J. Sammak, and D.E. Discher, "Physical plasticity of the nucleus in stem cell differentiation". *Proc. Natl. Acad. Sci. USA* 104, pp.15619-15624, 2007.

[39] Kong, F., A.J. Garca, A.P. Mould, M.J. Humphries, and C. Zhu, "Demonstration of catch bonds between an integrin and its ligand". *J Cell Biol.* 185, pp.1275-1284, 2009.

[40] Giannone, G. and M.P. Sheetz, "Substrate rigidity and force define form through tyrosine phosphatase and kinase pathways". *Trends Cell Biol.* 16, pp.213-23, 2006.

[41] Wang, N., J.D. Tytell, and D.E. Ingber, "Mechanotransduction at a distance: mechanically coupling the extracellular matrix with the nucleus". *Nat. Rev. Mol. Cell Biol.* 10, pp.75-82, 2009.

[42] Geiger, B., J.P. Spatz, and A.D. Bershadsky, "Environmental sensing through focal adhesions". *Nat. Rev. Mol. Cell Biol.* 10, pp.21-33, 2009.

[43] Valentine, M.T. , Z.E. Perlman, T.J. Mitchison, and D.A. Weitz, "Mechanical properties of Xenopus egg cytoplasmic extracts". *Biophys. J.* 88, pp. 680-689, 2005.

[44] Fabry, B. et al., "Scaling the microrheology of living cells". *Phys Rev Lett.* 87, pp.148102, 2001.

[45] Engler, A.J., "Embryonic cardiomyocytes beat best on a matrix with heart-like elasticity: scar-like rigidity inhibits beating". *J Cell Sci.* 121, pp.3794-3802, 2008.

[46] Krishnan, R. et al., "Reinforcement versus fluidization in cytoskeletal mechanoresponsiveness". *PLoS ONE* 4, pp.e5486, 2009.

[47] Zhou, J. et al., mTOR supports long-term self-renewal and suppresses mesoderm and endoderm activities of human embryonic stem cells. *Proc. Natl. Acad. Sci. USA* 106, pp.7840-7845, 2009.

[48] Chowdhury, F. et al., "Is cell rheology governed by nonequilibrium-to-equilibrium transition of noncovalent bonds?". *Biophys. J.* 95, pp.5719-5727, 2008.

[49] Panettieri, R.A., R.K. Murray, L.R. DePalo, P.A. Yadvish, and M.I. Kotlikoff, "A human airway smooth muscle cell line that retains physiological responsiveness". *Am. J. Physiol. Cell Physiol.* 25, pp.C329-C335, 1989.

[50] Bursac, P. et al., "Cytoskeletal remodelling and slow dynamics in the living cell". *Nat. Mater.* 4, pp.557-561, 2005.

[51] Kasza, K.E. et al., *Filamin A is essential for active cell stiffening but not passive stiffening under external force.* Biophys. J. 96, 4326-4335 (2009).

[52] Mijailovich, S.M., M. Kojic, M. Zivkovic, B. Fabry, and J.J. Fredberg, "A finite element model of cell deformation during magnetic bead twisting". *J. Appl. Physiol.* 93, pp.1429-1436, 2002.

[53] Viswanathan, S. et al., "Supplementation-dependent differences in the rates of embryonic stem cell self-renewal, differentiation, and apoptosis". *Biotechnol. Bioeng.* 84, pp.505-517, 2003.

[54] Vintersten, K. et al., "Mouse in red: red fluorescent protein expression in mouse ES cells, embryos, and adult animals". *Genesis* 40, pp.241-246, 2004.

[55] Pelham, R.J. Jr and Y. Wang, "Cell locomotion and focal adhesions are regulated by substrate flexibility". *Proc. Natl. Acad. Sci. USA* 94, pp.13661-13665, 1997.

[56] Wang, N. et al., "Cell prestress. I. Stiffness and prestress are closely associated in adherent contractile cells". *Am. J. Physiol. Cell Physiol.* 282, pp.C606-C616, 2002.

[57] Yeung, T. et al., "Effects of substrate stiffness on cell morphology, cytoskeletal structure, and adhesion". *Cell Motil. Cytoskeleton* 60, pp.24-34, 2005.

[58] Engler, A. et al., "Substrate compliance versus ligand density in cell on gel responses". *Biophys. J.* 86, pp.617-628, 2004.

Figure 2.1: Embryonic stemcells spread optimally on substrate of 0.6 **kPa**

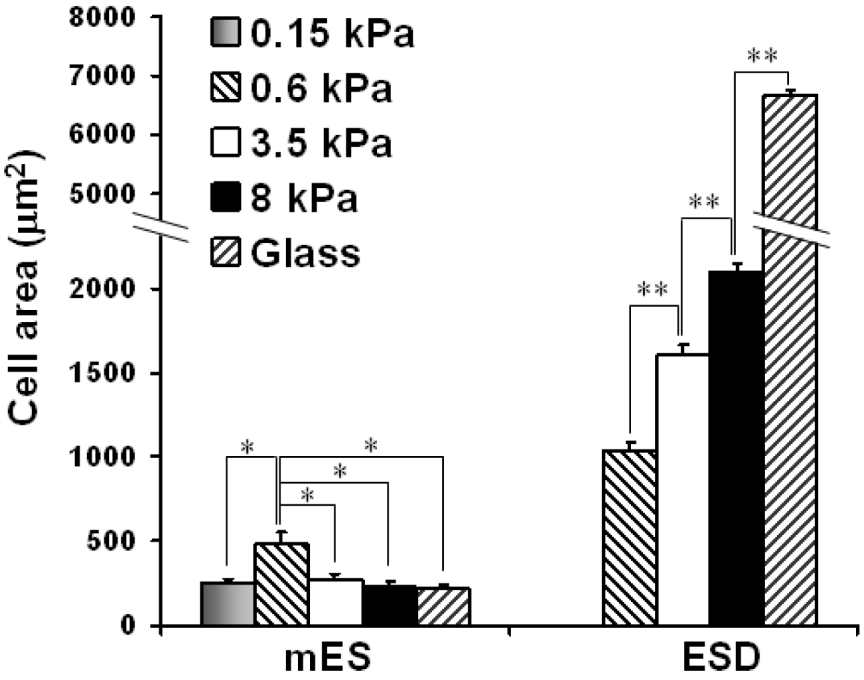

Cells were plated overnight on collagen-1 coated substrates with rigidity of 0.15-kPa, 0.6-kPa, 3.5-kPa, or 8-kPa polyacrylamide gel, or rigid glass. Left: *ES cells (n=9 cells for 0.15 kPa, 8 for 0.6 kPa, 7 for 3.5 kPa, 7 for 8 kPa, 12 for glass).* Right: *cells differentiated from ES cells (ESD) (n=12 cells for 0.6 kPa, 9 for 3.5 kPa, 8 for 8 kPa, 15 for glass). Means ± s.e.; at least three independent experiments. (* $p<0.05$; ** $p<0.001$). [From Chowdhury, F. et al. (2010) Nature Materials 9: 82- 88]*

Figure 2.2: mES cells are ∼10-fold softer than their differentiated counterpart ESD cells

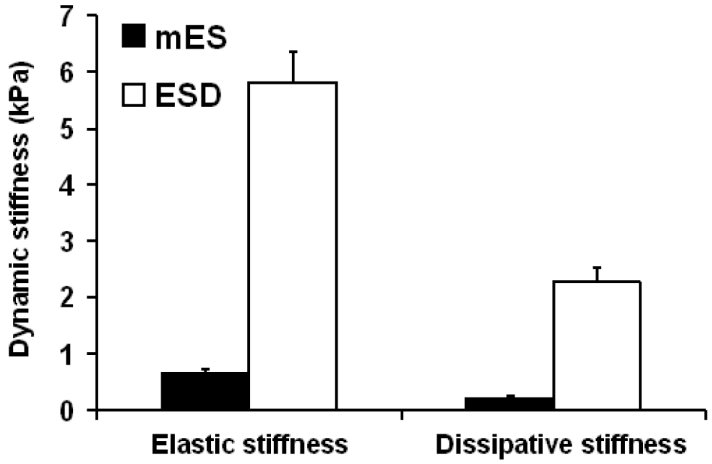

An oscillatory stress of 17.5 Pa at 0.3 Hz was applied to either ES cells or ESD cells via RGD-coated magnetic beads. Cells were plated overnight on collagen-1 (40 µg/ml) coated glass dishes. Although ES cells generally appear in lumps [48], their stiffness values do not change whether they are single individual cells or in lumps. In all our experiments, we chose to use only sparsely plated, single individual ES cells in order to precisely quantify cell area changes. The elastic stiffness or dissipative stiffness of the cells was computed [48]. n=∼200 mES cells, and n=∼250 ESD cells. At least 3 separate experiments. [Chowdhury, F. et al. (2008) Biophysical Journal 95: 5719- 5727 & Chowdhury, F. et al. (2010) Nature Materials 9: 82- 88]

Figure 2.3: mES cells but not ESD cells spread in response to a local cyclic stress

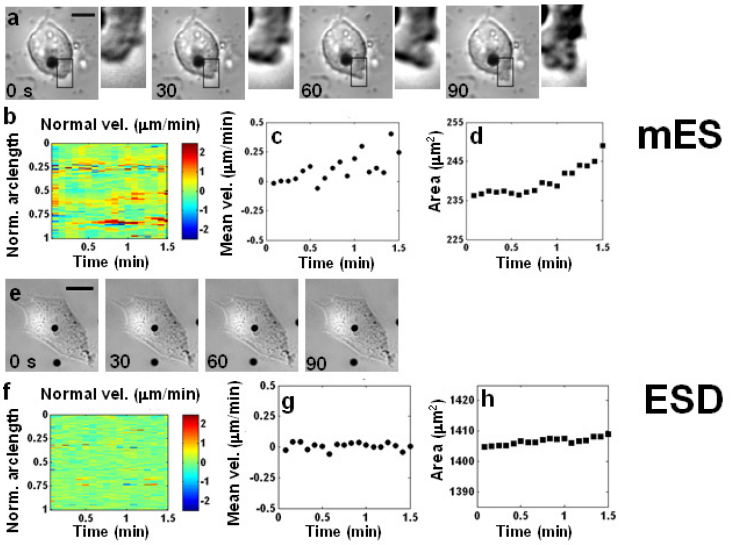

A mouse embryonic stem (mES) cell $(\mathbf{a}-\mathbf{d})$ *but not an embryonic stem cell-differentiated (ESD) cell* $(\mathbf{e}-\mathbf{h})$ *spreads in response to a local cyclic stress. A 4-μm RGD-coated ferromagnetic bead (the black dot) was attached to the apical surface of the cell for 15 min via integrins around. A local oscillatory stress of 17.5 Pa at 0.3 Hz was applied continuously.* **a**, *The applied stress induced a protrusion in an ES cell as early as 30 sec that grew with time (insets). (Scale bar, 10 μm.)* **b**, *Quantitative analyses of periphery movement velocity normal to the cell boundary in the ES cell (Normal vel; protrusion is shown as positive values; retraction is shown as negative values). The normal velocity is shown as a function of normalized arclength of the cell contour and time [24]. Note on the normal velocity map there are three visible hotspot bands indicating the spreading of ES cells induced by mechanical stress.* **c**, *Mean normal velocity around the ES cell periphery is shown as a function of time. A greater than zero value represents an overall spreading of the cell induced by the stress.* **d**, *Progressive protrusions around the cell periphery resulted in an increase in cell area of the ES cell.* **e**, *The ESD cell failed to spread in response to the same amplitude of mechanical stress. (Scale bar, 20 μm.)* **f**, *Normal velocity map of cell periphery indicates that the ESD cell was relatively quiescent and unresponsive.* **g**, *Mean normal velocity of the ESD cells was zero over time, suggesting lack of response to the mechanical stress.* **h**, *No change in the projected area of the ESD cell was observed over time. In general, mES cells form colonies. mES cells in a colony also spread in response to a local cyclic stress (17.5 Pa at 0.3 Hz) (see Fig. 2.14), suggesting that our findings on individual single cells are applicable to a colony of mES cells. [Chowdhury, F. et al. (2010) Nature Materials 9: 82- 88]*

Figure 2.4: Cell softness dictates cell spreading response to stress

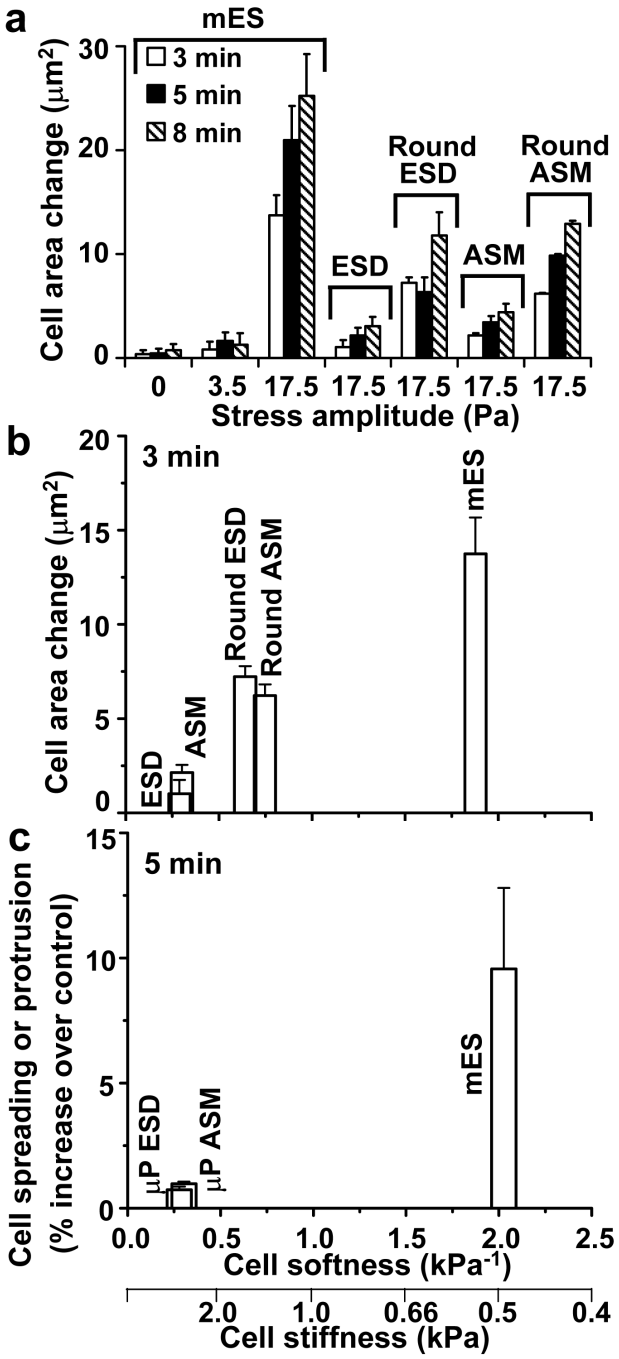

a, *spreading in mES cells is amplitude-dependent. Amplitude is the magnitude of change in a sinusoidal oscillatory forcing system where the mean magnitude is zero. ES cells did not spread at 0 or 3.5-Pa stress but started to protrude and spread at 17.5-Pa stress (n=7, 5, or 9 cells for 0, 3.5, or 17.5 Pa stress, respectively). There were no significant differences in cell*

area change between 0 and 3.5-Pa stress ($p>0.58$, 0.23, or 0.68 at 3, 5, or 8 min). In contrast, there were significant differences between 3.5 and 17.5 Pa stress ($p<0.0007$, 4.92×10^{-5}, or 5.66×10^{-5} at 3, 5 or 8 min respectively). At 17.5 Pa stress, there was significant difference in cell area between 3 min and 5 min ($p<0.05$), but no significant difference in cell area between 5 min and 8 min ($p>0.23$). In sharp contrast, for ESD cells and ASM cells there were no stress-induced changes in cell area even at 17.5-Pa applied stress ($n= 7$ cells for both cell types). There were no significant differences in cell area change between 3 min and 5 min ($p>0.30$ for ESD and $p>0.09$ for ASM) or 5 min and 8 min ($p>0.47$ for ESD and $p>0.37$ for ASM). Round ESD cells and round ASM cells spread but to a lesser degree than mES cells (Fig. 2.18). (Means ± s.e.; at least 3 independent experiments) **b**, *Stress-induced cell spreading depends on cell softness. mES cells, ESD, and ASM cells were plated on similar culture conditions (high density of collagen-1, 100 μg/ml) and on the same substrate stiffness of 0.6 kPa. The change in cell area of ESD and ASM cells is statistically different from mES cells at 3 min ($p<0.05$). Round ESD and round ASM cells were plated on low density of collagen-1 (1 ng/ml) coated on the rigid glass. Changes in cell area (spreading) after 3 min of stress application (17.5 Pa at 0.3 Hz) were plotted. Note that stress-induced cell spreading appears to be proportional to cell softness. Cell softness correlates inversely with F-actin density in each cell type (see Fig. 2.6). Mean ± s.e., n=7, 9, 7, 7, and 9 for ESD, round ESD, ASM, round ASM, and mES cells respectively.* **c**, *Cell softness, rather than cell projected area, dictates spreading or protrusion responses to stress. Each ESD cell or ASM cell was plated on a micropattened adhesive island (25-μm diameter circles) on 0.6 kPa substrate stiffness coated with 100 μg/ml of type-1 collagen and thus was restricted to within an area of ∼500 μm^2. The gel surface outside the islands was uncoated and thus was nonadhesive. No visible protrusion on the micropatterned ESD and ASM cells (μP ESD and μP ASM) was observed when stressed for 5 min. The data of μP ESD and μP ASM cells are significantly different from those of mES cells at 5 min ($p<0.006$ and $p<0.007$ respectively). Mean ± s.e., n=5, 5 and 9 for μP ESD, μP ASM and mES cells respectively. [Chowdhury, F. et al. (2010) Nature Materials 9: 82- 88]*

Figure 2.5: Stress-induced early spreading in ES cells is stress frequency dependent

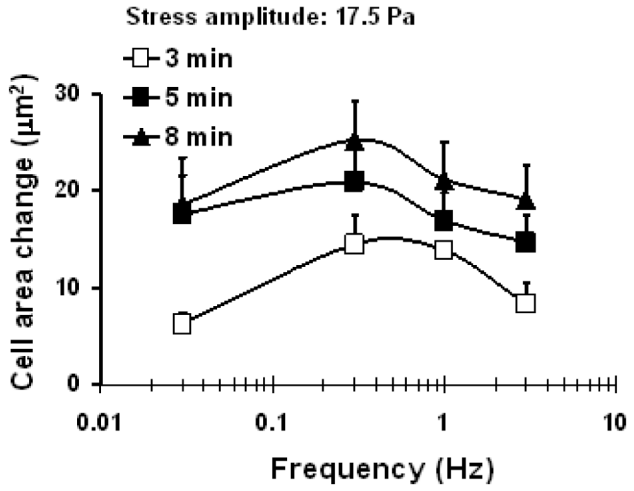

Stress amplitude was fixed at 17.5 Pa. Three minutes after loading, there were significant differences in cell area changes between 0.03 and 0.3 Hz ($p<0.01$) and between 1 and 3 Hz ($p<0.03$) but no difference between 0.3 and 1 Hz ($p>0.48$). At later times after onset of loading (5 and 8 min), there were no differences in cell areas between different frequencies. In contrast to 3 min loading in which loading frequency is optimal at 0.3-1 Hz, at 5 min loading, there were no significant differences: $p>0.20$ between 0.03 and 0.3 Hz; $p>0.09$ between 0.3 and 1 Hz; $p>0.59$ between 1 and 3 Hz respectively. At 8 min, there were no significant differences: $p>0.10$ between 0.03 and 0.3 Hz; $p>0.15$ between 0.3 and 1 Hz; $p>0.69$ between 1 and 3 Hz respectively. $n=6$, 9, 8, or 9 cells at 0.03, 0.3, 1, or 3 Hz respectively (three separate experiments). [Chowdhury, F. et al. (2010) Nature Materials 9: 82- 88]

Figure 2.6: F-actin distribution in mES cells, ESD cells, and round ESD cells on low matrix proteins (1 ng/ml collagen-1)

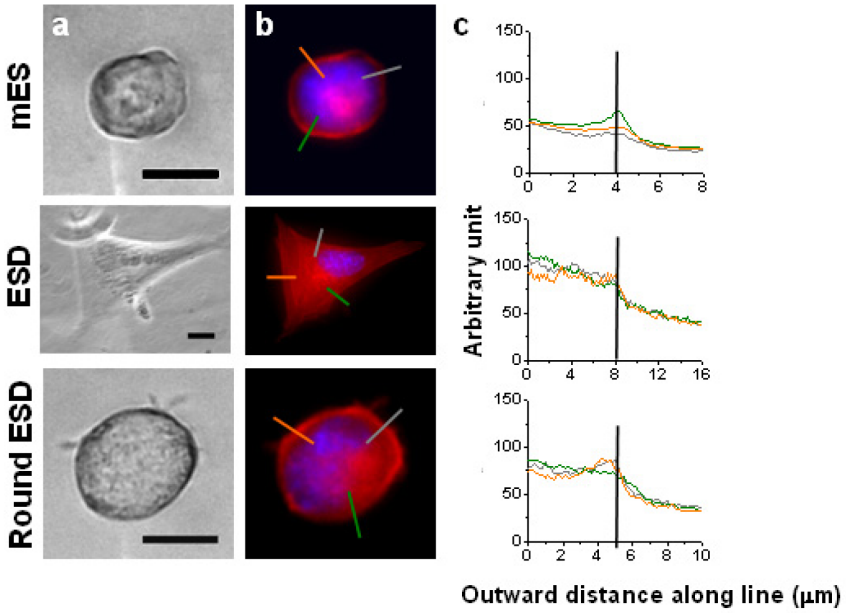

a, *Phase contrast images of representative mES, ESD, or round ESD cell.* **b**, *Cells were stained with rhodamin-phalloidin for F-actin (red) and Hoechst 33342 for DNA (blue). Three color lines were arbitrarily selected for quantifying F-actin fluorescent intensity at 3 different cytoplasm regions.* **c**, *F-actin fluorescent intensities along the 3 color lines in each cell. The F-actin densities are lowest in the mES cell, medium in the round ESD cell, and highest in the spread ESD cell. The F-actin densities appear to be inversely correlated with cell softness and consistent with the mechanical data of these cells in Fig. 2.4b. Solid vertical lines represent cell edges. (Scale bar, 15 μm.) [Chowdhury, F. et al. (2010) Nature Materials 9: 82- 88]*

Figure 2.7: Stress-induced spreading in mES cells correlates with accumulation of phosphorylated myosin light chain and elevation of tractions at the cell edge

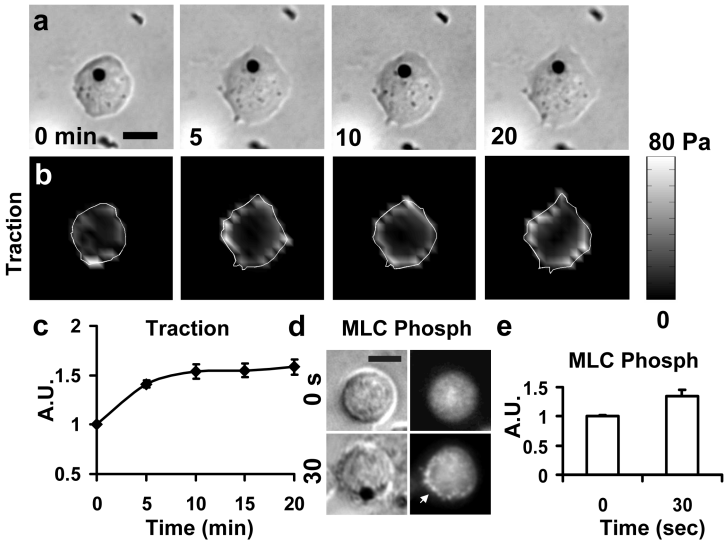

a, *A brightfield image shows the time course of a mES cell spreading in response to the applied stress (17.5 Pa at 0.3 Hz).* **b**, *Corresponding traction in the same ES cell in response to the applied stress.* **c**, *Average tractions at 1-μm annulus around the cell boundary as a function of time after stress application. A.U.=arbitrary unit, tractions normalized by the traction at zero applied stress. n=8 cells, mean±s.e.* **d**, *Phosphorylated myosin light chain (MLC Phosph) was accumulated to the cell periphery (white arrow) 30 s after stress application in comparison to a diffuse cytoplasmic distribution at time zero.* **e**, *Phosphorylated myosin light chain at 1-μm annulus around the cell boundary. A.U.=arbitrary unit, normalized by the values at zero applied stress. n=23 and 11 cells for 0 and 30 sec respectively; mean ± s.e. (Scale bar, 15 μm.) [Chowdhury, F. et al. (2010) Nature Materials 9: 82- 88]*

Figure 2.8: Stress-induced ES cell spreading depends on myosin II activity, Src, Cdc42, but not on Rac activity

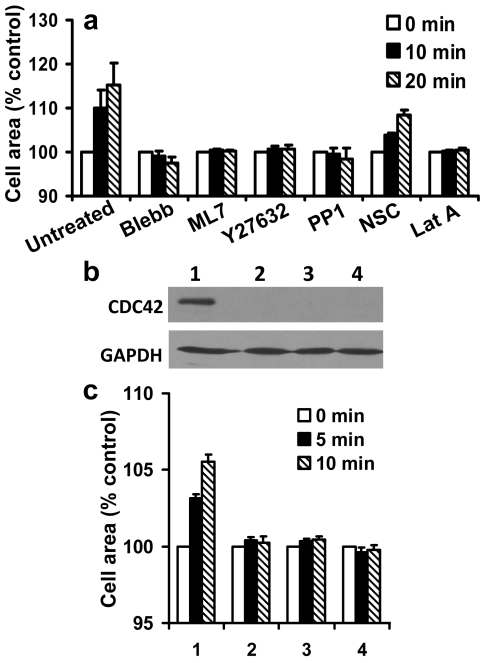

a, *Summarized data after drug treatments were compared with those of untreated cells (n=5 cells). Control = cell areas before stress application. Inhibiting myosin II ATPase with Blebbistatin (50 μM for 30min; n=7 cells), inhibiting myosin light chain kinase with ML7 (25 μM for 20min; n=5 cells), inhibiting ROCK with Y27632 (50 μM for 20min; n=5 cells), or inhibiting Src activity with PP1 (10 μM for 1hr; n=5 cells), all prevented stress-induced cell spreading, i.e., no significant changes in cell areas between 0 and 10 min and between 0 and 20 min ($p>0.05$). For inhibiting Rac with NSC23766 (100 μM for 1hr; n=5 cells), there were significant changes in cell areas ($p<0.006$ and $p<0.0009$) between 0 and 10 min and between 0 and 20 min. Latrunculin A (0.1 μg/ml for 30 min) (n=10 cells) to disrupt F-actin also prevented stress-induced spreading. Mean ± s.e.* **b**, *Cdc42 is necessary for stress-induced spreading in mES cells. Western blots of Cdc42 in mES cells under different conditions. Lane 1, non-target shRNA control; Lane 2-4, different constructs to knockdown Cdc42. An independent experiment showed similar results.* **c**, *Corresponding changes in cell areas after stress application after Cdc42 knockdown (17.5 Pa at 0.3 Hz). n=9, 8, 9, 8 cells for Lane 1-4 respectively; mean ± s.e. (for Lane 1, $p < 8.68\times10^{-7}$ and $p < 2.66\times10^{-6}$ comparing between 0 and 5 min, 0 and 10 min; there were no significant changes ($p>0.05$) for Lane 2 through Lane 4). Note that cdc42 knockdown correlated strongly with abolishment of stress-induced spreading response, suggesting that Cdc42 is critical in stress-induced protrusion and spreading. [Chowdhury, F. et al. (2010) Nature Materials 9: 82- 88]*

Figure 2.9: Phase contrast images of representative mES cells in response to stress after different drug treatments

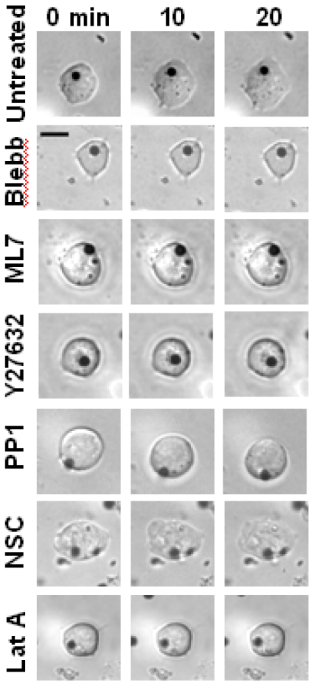

Untreated: control cell; Blebb: Blebbistatin (50 μM for 30min) to inhibit myosin II ATPase; ML7 (25 μM for 20min) to inhibit myosin light chain kinase; Y27632 (50 μM for 20 min) to inhibit ROCK;, PP1 (10 μM for 1hr) to inhibit Src; NSC: NSC23766 (100 μM for 1 hr) to inhibit Rac; Lat A: Latrunculin A (0.1 μg/ml for 30 min) to disrupt actin microfilaments. Clearly stress-induced spreading in mES cells are dependent on myosin II, F-actin, ROCK and Src, but not on Rac activity. (Scale bar, 15 μm applies to all cells) [Chowdhury, F. et al. (2010) Nature Materials 9: 82- 88]

Figure 2.10: Nonspecifically stressing mES cells with Poly-L-lysine coated beads did not induce cell spreading

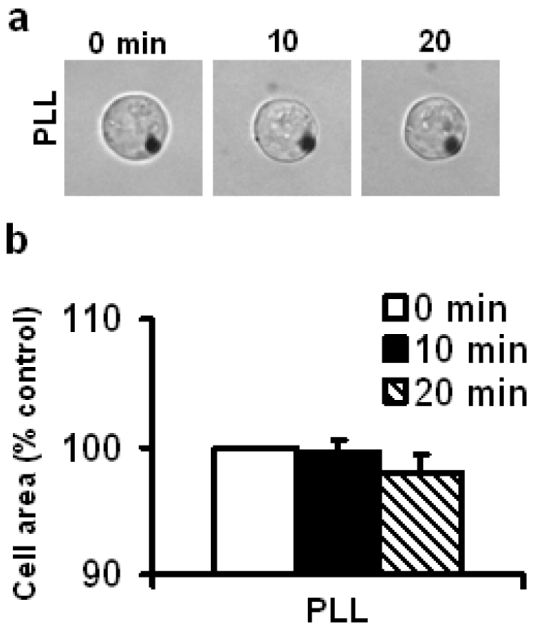

For deforming the cell nonspecifically with poly-l-lysine coated beads (n=5; 17.5 Pa stress at 0.3 Hz), there were no significant changes in cell areas ($p>0.70$ and >0.21) between 0 and 10 min and between 0 and 20 min, suggesting that stress-induced spreading in mES cells is specific via integrins. Means ± s.e. are from at least two independent experiments. [Chowdhury, F. et al. (2010) Nature Materials 9: 82- 88]

Figure 2.11: Knocking out Cdc42 blocks stress-induced spreading in mES cells

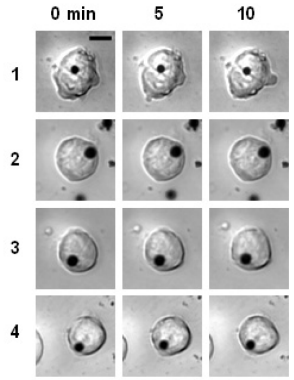

1, Non-target shRNA Control
2, TRCN0000071684: CCGGCTGTCCAAAGACTCCTTTCTTCTCGAGAAGAAAGGAGTCTTTGGACAGTTTTTG
3, TRCN0000071686: CCGGCCGCTAAGTTATCCACAGACACTCGAGTGTCTGTGGATAACTTAGCGGTTTTTG
4, TRCN0000071683: CCGGCGGAATATGTACCAACTGTTTCTCGAGAAACAGTTGGTACATATTCCGTTTTTG

Procedures were described in Methods. Corresponding sequences of shRNA for Cdc42 were shown: Lane 1, non-target shRNA control; Lane 2-4, different constructs to knockdown Cdc42. It appears that knockdown of Cdc42 shRNA in Lane 2-4 completely prevented stress-induced spreading. (Scale bar, 10 μm.) [Chowdhury, F. et al. (2010) Nature Materials 9: 82- 88]

Figure 2.12: A local cyclic stress substantially diminishes OCT3/4 expression in mES cells

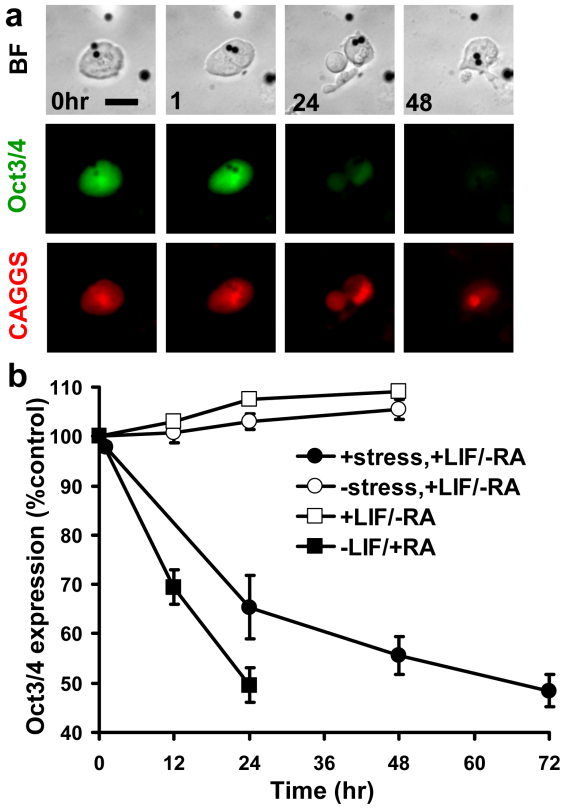

a, *Brightfield (BF) images (top), corresponding GFP images of OCT3/4 expression (middle), and corresponding DsRed images of a constitutive promoter (CAGGS) expression (bottom), all from the same cell(s), are shown over time. Cells attached to RGD-coated beads (black dots) were continuously stressed for ∼1 hr (17.5 Pa at 0.3 Hz) and OCT3/4 expression or CAGGS expression was measured over time in the homogeneous pluripotent mES cells (assessed by the uniform high GFP fluorescent intensity in all mES cells, unique cell shapes, and colony forming capability) plated on high density collagen-1 (100 μg/ml) coated 0.6 kPa substrate. (Scale bar, 10 μm.)* **b**, *Summarized data for the cells in mES cell culture medium that were exposed to stress (+stress, +LIF/-RA; closed circles, n=5), the cells in the same dish but were not stressed (stress, +LIF/-RA; open circles, n=9), the cells in mES cell culture medium in separate dishes (+LIF/-RA; open squares, n=9), and the cells in the differentiation medium (LIF/+RA; closed squares, n=10) are shown here. OCT3/4 expression is normalized with respect to time zero (control). Mean ± s.e.; two independent experiments. [Chowdhury, F. et al. (2010) Nature Materials 9: 82- 88]*

Figure 2.13: Representative fluorescent images of OCT3/4 expression under three different conditions

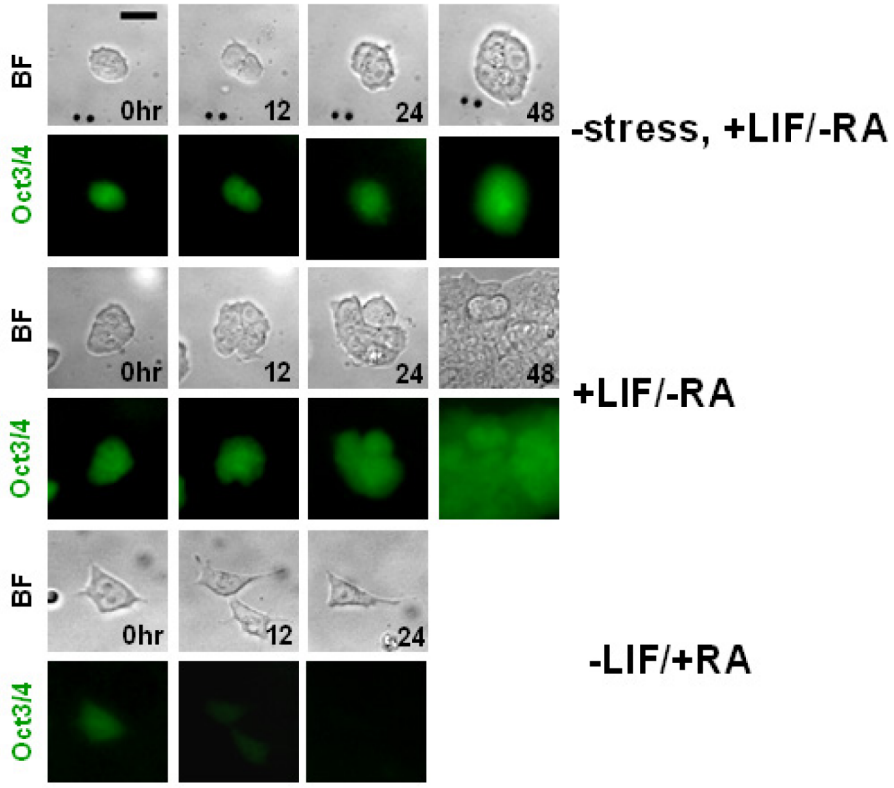

Top: stress, +LIF/-RA, the cell was in the same dish as +stress, +LIF/-RA condition. Middle: +LIF/-RA, the cell was in a different dish. Bottom: LIF/+RA, the cell was in the differentiation medium. OCT3/4 expression increased over time for stress, +LIF/-RA and +LIF/-RA conditions, whereas it drastically decreased for LIF/+RA condition. Down-regulation of OCT3/4 by RA was quick because of a retinoic acid receptor binding domain in the regulatory region of OCT3/4. (Scale bar, 10 μm.) [Chowdhury, F. et al. (2010) Nature Materials 9: 82- 88]

Figure 2.14: mES cells in a colony also spread in response to a local cyclic stress

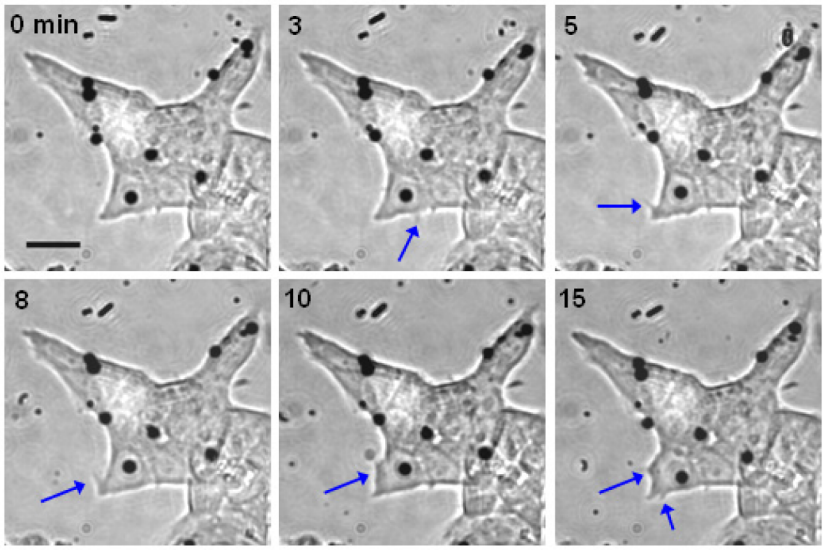

mES cells in a colony also spread in response to a local cyclic stress (17.5 Pa at 0.3 Hz) via a RGD-coated magnetic bead. Blue arrows point to the sites of cell protrusion. Black dots are RGD-coated magnetic beads. The cell area increased significantly after 10-15 min of stress application. (Scale bar, 20 μm.) [Chowdhury, F. et al. (2010) Nature Materials 9: 82- 88]

Figure 2.15: Stress-induced spreading in mES cells occurs in the absence of serum

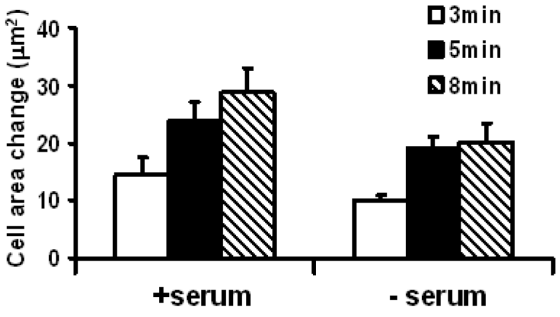

Compared with the mES cells cultured in 1% serum, mES cells cultured in zero serum also responded to a local cyclic stress (17.5 Pa at 0.3 Hz), although the extent of spreading was somewhat less, especially at longer times (8 min). n= 9 and 8 for 1% serum and no serum condition respectively. There were no significant differences in cell area change between 1% serum and no serum for 3, 5 and 8 min ($p>0.05$). Mean ± s.e. Two separate experiments. [Chowdhury, F. et al. (2010) Nature Materials 9: 82- 88]

Figure 2.16: Quantification of magnetic bead embedment in mES cells

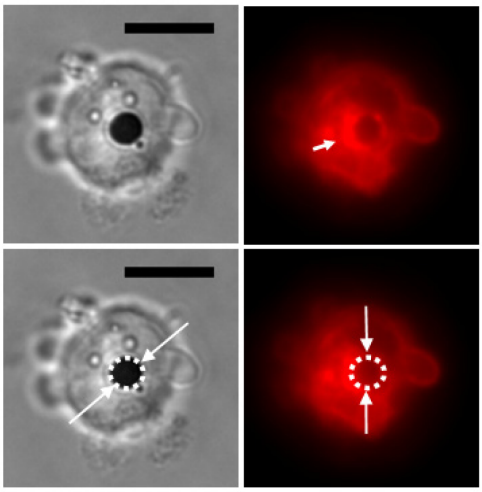

An RGD-coated magnetic bead was bound to the apical surface of the mES cell for 15 min. Then the cell was fixed and stained with rhodamine-phalloidin. The recruitment of actin surrounding the bead (small white arrow) was due to the formation of an integrin-mediated focal adhesion at the bead-cell surface contact. By measuring the maximum actin ring diameter from the fluorescent image and the maximum bead diameter from the brightfield image (large white arrows), one can estimate the bead embedment in the cell. This representative cell shows ∼50% embedment of the bead. (Scale bar, 15 μm.) [Chowdhury, F. et al. (2010) Nature Materials 9: 82- 88]

Figure 2.17: Stress-induced spreading of mES cells at different times

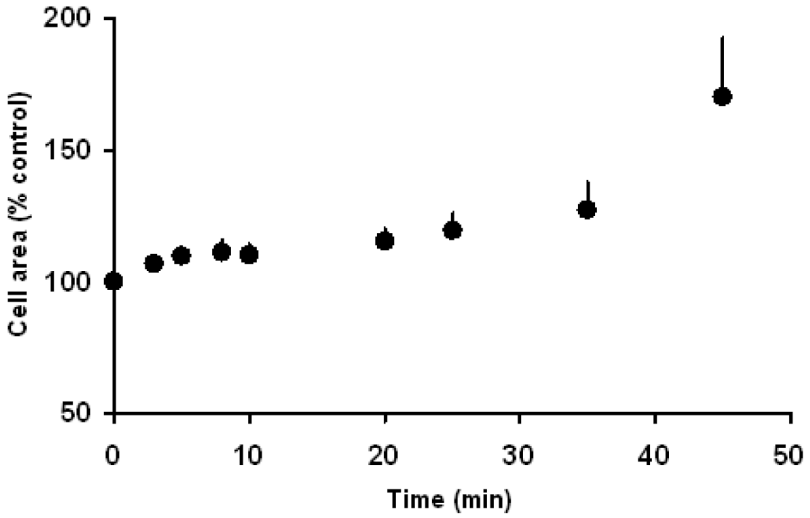

A local cyclic stress (17.5 Pa at 0.3 Hz) was applied for different durations up to 45 min. Cell areas increase by 65% at 45 min. n=9 for each data point, up to 8 min; n=5 from 10 min to 45 min. Mean ± s.e. are from at least 3 independent experiments. [Chowdhury, F. et al. (2010) Nature Materials 9: 82- 88]

Figure 2.18: Round ESD and round ASM cells exhibit stress induced protrusion

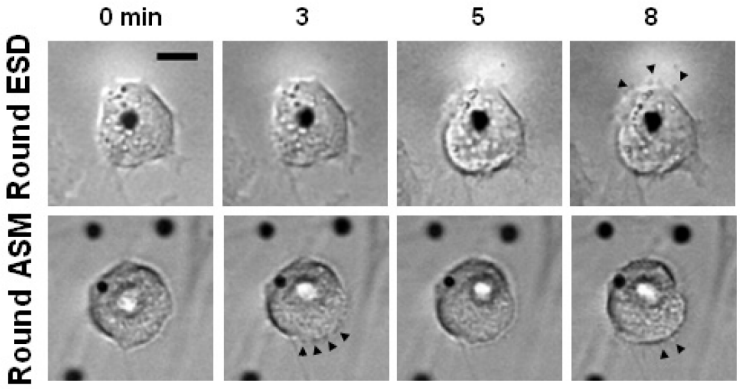

A representative round ESD cell or round ASM cell, plated on low concentration of type I collagen (1 ng/ml), exhibits stress-induced protrusion and spreading (arrowheads), similar to an mES cell. (Scale bar, 10 µm.) [Chowdhury, F. et al. (2010) Nature Materials 9: 82- 88]

CHAPTER 3

DOWNREGULATING CELL-MATRIX TRACTIONS PROMOTE HOMOGENEOUS SELF-RENEWAL OF EMBRYONIC STEM CELLS

Adapted from Chowdhury et al. (2010) PLoS ONE 5(12): e15655

3.1 Abstract

Maintaining undifferentiated mESC culture has been a major challenge as mESCs cultured, even in the presence of LIF, exhibit spontaneous differentiation, fluctuating expression of pluripotency genes, and genes of specialized cells. Here we show that, in sharp contrast to the mESCs seeded on the conventional rigid substrates, the mESCs cultured on the soft substrates that match the intrinsic stiffness of the mESCs and in the absence of exogenous LIF for 5 days, surprisingly still generated homogeneous undifferentiated colonies, maintained high levels of OCT3/4, NANOG, and Alkaline Phosphatase (AP) activities, and formed embryoid bodies and teratomas efficiently. A different line of mESCs, cultured on the soft substrates without exogenous LIF, maintained the capacity of generating homogeneous undifferentiated colonies with relatively high levels of OCT3/4 and AP activities, up to at least 15 passages, suggesting that this soft substrate approach applies to long term culture of different mESC lines. mESC colonies on these soft substrates without LIF generated low cell-matrix tractions and low stiffness. Both tractions and stiffness of the colonies increased with substrate stiffness, accompanied by downregulation of OCT3/4 expression. Our findings demonstrate that mESC self-renewal and pluripotency can be maintained homogeneously on soft substrates via the biophysical mechanism of facilitating generation of low cell-matrix tractions.

Key words: cell stiffness, substrate stiffness, traction forces, differentiation, pluripotency

3.2 Introduction

Embryonic stem cells are artificial stem cells that have adapted to the in vitro culture environment. Since the first isolation of mouse mESCs in 1981, mESCs have served as an excellent model to understand the mechanism of cell fate decision in developing embryos. However, the research encounters unrelenting challenges in keeping them undifferentiated homogeneously and directing their specific differentiation in vitro. Many studies over the years have demonstrated that undifferentiated mESC culture contains heterogeneous populations which are identified by fluctuating expression of transcripts and cell-surface markers [1-10]. Thus, well-accepted culture conditions are limited in maintaining self-renewal and pluripotency of mESCs [11-13] and human ESCs (hESCs) [14-16]. The importance of physical microenvironments in regulating stem cell differentiation is becoming evident nowadays [17-23]. Recently, we have demonstrated that mESCs are intrinsically soft and respond optimally to physical forces when cultured on substrates that match their intrinsic softness [24]. Here we demonstrate that mESCs maintain their pluripotent state optimally on the soft matrix via the mechanism of generating low cell-matrix tractions and low stiffness.

3.3 Results

3.3.1 Culturing mESCs on soft substrates generates homogeneous colonies

To explore the potential role of substrate stiffness on mESC self-renewal, we plated mESCs on soft substrates of 0.6 kPa polyacrylamide gels (referred to gels hereafter) that matches the intrinsic mESC stiffness or on rigid substrates of polystyrene dishes (stiffness $>$ 4 MPa) [25]; both were coated with of type-1 collagen (collagen-1), which is known to facilitate mESC self-renewal [26], under the standard culture conditions including LIF and animal serum. These mESCs express EGFP under the OCT3/4 (Pou5f1) promoter (OCT3/4::GFP; ref. 27). As the mESCs were continuously cultured to form colonies, round and compact colonies were formed uniformly on the gels (precoated with 100 μg/ml type I collagen) with high OCT3/4::GFP expression

and high alkaline phosphatase (AP) activities (Fig. 3.1a). In contrast, the mESCs plated on rigid dishes (pre-coated with 40 μg/ml type I collagen) exhibited appearances of heterogeneous colony shapes, and varying levels of OCT3/4::GFP expression and AP activity (Fig. 3.1b). Similar results were obtained when mESCs were plated on rigid dishes coated with 100 μ g/ml collagen-1 (Fig. 3.2), suggesting that these colonies heterogeneous shapes and low levels of OCT3/4 expression and AP activity are due to the rigidity of the dishes, and not due to the number of the attached collagen-1 molecules. These data were confirmed in freshly thawed mESCs: on soft substrates (Fig. 3.3c, d), homogenous round and compact colonies corresponded to high expressions of OCT3/4::GFP (Fig. 3.3c$'$, d$'$), whereas mESCs plated directly on rigid dishes generated heterogeneous colonies of varying shapes (Fig. 3.3a, b), corresponding to varying expression levels of OCT3/4::GFP (Fig. 3.3a$'$, b$'$). Interestingly, the mESCs plated on mouse embryonic fibroblast (MEF) feeder cells exhibited various shapes of colonies ranging from very round to somewhat flattened (Fig. 3.3e, f), corresponding to heterogeneous expression levels of OCT3/4::GFP (Fig. 3.3e$'$, f$'$). The differences in colony shapes and OCT3/4 expression between the mESCs on soft substrates and the mESCs on MEFs may be resulted from the fact that MEFs are much stiffer ($\sim$10-fold) than mESCs [28]. To compare different shapes between colonies on different substrates, we measured the shape factor of mESC colonies and found that mESCs on the soft gels are much more circular than those on the rigid dishes or on the feeder cells (Fig. 3.3g). To further explore the effect of the substrate stiffness on mESC culture, we withdrew LIF from the culture for 3 days (LIF- 3 days). Interestingly, mESCs cultured on the gels were still capable of forming round and compact colonies with the OCT3/4::GFP expression and the AP activity was maintained (Fig. 3.1c); remarkably, even in the absence of LIF for 5 days (LIF- 5 days), mESCs on gels still maintained high levels of OCT3/4::GFP, NANOG, and the AP activity (Fig. 1e, g). In sharp contrast, the mESCs on rigid substrates in LIF- 3 days started to exhibit signs of cell differentiation with significantly reduced OCT3/4::GFP expression and the AP activity (Fig. 3.1d); as expected, in LIF- 5 days, these mESCs exhibited appearances of differentiated cells with no detectable AP activity, nor OCT3/4 and NANOG expression (Fig. 3.1f, h). These data show that soft substrates can override the LIF-Stat3 signaling pathway for at least 5 days in maintaining mESC self-renewal. Next, we compared the per-

centage of OCT3/4::GFP-positive mESCs cultured on the gels with those on rigid substrates. Remarkably, almost all mESCs (92%) cultured on the soft gels maintained high OCT3/4::GFP expression levels in LIF- conditions (Fig. 3.4 a-g), similar to those in LIF+ conditions (93%) ($p=0.83$). In contrast, when LIF was withdrawn from the culture of mESCs on rigid substrates for 5 days, OCT3/4::GFP-positive mESCs significantly decreased (from 94% to 59%, $p<0.029$; Fig. 3.4a-g). Taken together, these results indicate that the substrate stiffness is a crucial extrinsic factor to sustain the self-renewal of mESCs.

3.3.2 Pluripotency of mESCs is maintained on soft substrates

Because mESCs can self-renew efficiently on soft substrates, we asked whether mESCs cultured on soft substrates are still pluripotent or not. The efficiency of these mESCs to form embryoid bodies (EBs) from hanging drops was examined [29]. There were no significant differences in the efficiencies of EB formation for mESCs on soft gels with or without LIF ($p>0.25$); more than 90% of the hanging drops made with the mESCs formed EBs. In sharp contrast, EBs were formed in only 77% of the drops made with the mESCs maintained on rigid substrates without LIF, compared with more than 90% of the drops with the mESCs cultured on rigid substrates with LIF ($p<0.01$, Fig. 3.5a). Next, we examined expression of genes associated with the undifferentiated state of mESCs (OCT3/4, SOX2, NANOG, ESG1/DPPA5, and TCF15) as well as the genes associated with cell differentiation (TWIST2 and T/Brachyury; ref. 30) in mESCs cultured on the soft gel or on the rigid substrate with or without LIF (Fig. 3.5b). Semi-quantitative reverse transcriptase-polymerase chain reaction (RT-PCR) data demonstrated that, in the presence of LIF (LIF+), there were no significant differences between the mESCs cultured on the gels and rigid substrates (Fig. 3.5b, top). However, in the absence of LIF for 5 days (LIF-), the mESCs on the soft gel still maintained high expression levels of OCT3/4, SOX2, ESG1 and TCF15, which were significantly downregulated in the mESCs on the rigid substrate (Fig. 3.5b, bottom). Cell differentiation was evident in the mESCs on the rigid substrate because the early mesodermal marker, T, was upregulated dramatically (Fig. 3.5b, bottom). However, TWIST2, a late mesodermal

marker, was not activated in mESCs on either the soft gels or the rigid substrates (Fig. 3.5b, bottom), consistent with the fact that the mESCs on the rigid substrates without LIF were in the very early stages of differentiation. Noticeably, the high expression level of the gene responsible for tumorigenic growth of mESCs, Eras [31], was still maintained in the mESCs on the soft gel in LIF- conditions (Fig. 3.5b, middle). This finding led to our investigation into the formation of teratomas by these mESCs. When mESCs on the soft gel with LIF were transplanted to NOD-SCID mice subcutaneously for 6 weeks, they grew into a well-developed teratoma (Fig. 3.6a, dashed-circles) with cell types of three germ layers (Fig. 3.6c-e). As expected, teratomas were formed when the mESCs on the rigid substrate with LIF were transplanted. Intriguingly, when the mESCs maintained on the gels without LIF for 5 days were transplanted for 7 weeks, they were able to grow into a well-developed teratoma (Fig. 3.6b, dashed-circle on the left) consisting of cell types of three germ layers, much larger than the teratoma generated from the mESCs on the rigid substrate without LIF (Fig. 3.6b, dashed-circle on the right). This result is consistent with the high expression level of Eras in the mESCs on the soft gel without LIF and the low expression level of Eras in the mESCs on the rigid substrate without LIF (Fig. 3.5b). To determine if our approach could be extended to other mESC lines and for long term cultures, we initiated culture of another established line of mESCs (W4, 129/SvEv). Remarkably, after W4 mESCs were passaged more than 15 times on the soft gels without exogenous LIF continuously for more than 2 months, they still exhibited round, compact colonies with relatively high levels of OCT3/4 expression and the AP activity (Fig. 3.7, row 3). In contrast, W4 mESCs cultured on the rigid dishes for the same duration, even in the presence of LIF, exhibit irregular shapes of colonies with some differentiated cells at the periphery of the colony and with low levels of AP activity and OCT3/4 expression (Fig. 3.7, row 1). These results demonstrate that the soft substrate strategy to promote self-renewal of ESCs could be applied to other mESCs for long term cell cultures.

3.3.3 A biophysical mechanism of substrate softness mediated mESC self-renewal

Increasing evidence suggests that matrix substrate rigidity influences cell functions via a biophysical mechanism [18, 19]. To explore the biophysical mechanism of mESC self-renewal on soft substrates, we plated mESCs on 0.6 kPa (soft), 3.5 kPa (relatively stiff), or 8 kPa (stiff; ∼10-fold greater than the intrinsic mESC stiffness) substrates in the presence or absence of LIF and allowed individual cells to grow into colonies. As observed earlier, mESCs on 0.6 kPa substrates formed round compact colonies (Fig. 3.8a), maintained high OCT3/4::GFP, with or without LIF (Fig. 3.8b). Tractions on the basal surface and stiffness on the apical surface of the colony did not change with or without LIF on the 0.6 kPa soft substrate (Fig. 3.8c-e). However, as the substrate stiffness increased from 0.6 to 3.5, and then to 8 kPa, the mESC colonies with LIF became irregular and expressed low levels of OCT3/4 (Fig. 3.8a, 3.8b). The shapes of the colonies on the 8 kPa substrate are similar to those from the mESC colonies on the rigid substrate of polystyrene dishes, suggesting that the 8 kPa substrate and the rigid substrate are equivalent in rigidity in regards to mESC stiffness: stiffnesses of both substrates are much higher than mESC stiffness. The mESC colonies on 3.5 kPa substrates with LIF generated higher tractions and higher stiffness than on 0.6 kPa substrates with LIF, but similar tractions as those on 8 kPa substrates (Fig. 3.8c-e). This result suggests that mESCs have started to respond mechanically (changes in traction and stiffness) and biologically (changes in OCT3/4 expression) when the substrate stiffness is increased by as little as a factor of 6 (from 0.6 to 3.5 kPa). In LIF- conditions for 5 days, the mESC colonies on 8 kPa substrates, similar to those on 3.5 kPa substrates, became much more spread and irregular, showing signs of differentiation (Fig. 3.8a), and significantly elevated their tractions and stiffness (Fig. 3.8c-e), accompanied by diminishing OCT3/4 expression (Fig. 3.8b). To further examine the role of myosin II in traction generation of the colonies, we cultured mESCs on 8 kPa substrates with blebbistatin (10 μM) for 5 days. After treatment with blebbistatin to inhibit myosin II, the colonies became much more uncompact and irregular (Fig. 3.9a, b), and tractions were downregulated (Fig. 3.9c, d). Addition of blebbistatin significantly lowered the levels of OCT3/4 expression in the colonies without LIF from the control (untreated cells with LIF). These

data are consistent with a recent report that blebbistatin treatment decreases compactness and slightly downregulates OCT3/4 expression of human ESC (hESC) colonies [32]. Together with the published reports that mouse embryos cease to develop when myosin-IIs are genetically knocked out [33,34], differentiation of mesenchymal stem cells directed by matrix substrates is blocked when myosin-II-dependent tractions are inhibited [17], and external stress-induced mESC spreading and differentiation are inhibited by myosin-II inhibitor blebbistatin [24], our present data demonstrate that mESC colonies on soft substrates maintain their self-renewal and pluripotency via the biophysical mechanism of generating low cell-matrix tractions and low stiffness.

3.4 Discussion

Our data show that when the stiffness of matrix substrates matches that of the soft mESCs, the soft substrate promotes self-renewal and pluripotency of mESCs, even in the absence of LIF for at least 5 days. These results demonstrate that the substrate softness plays a crucial role in the maintenance of mESC self-renewal and pluripotency. It is clear from our data that our approach can generate homogeneous mESC culture, a major advantage over the standard culture approach. Importantly, plating mESCs on soft substrates is able to override the differentiation propensity triggered by LIF withdrawal from the medium. Our discoveries on the importance of matching the material properties of the substrate with those of the mESCs on the optimal mESC self-renewal and pluripotency functions extend the previous findings in skeletal and cardiac muscle cells [35,36] and the finding from a very recent report on skeletal muscle stem cells [37]. The generation of a homogeneous undifferentiated population of all mESC colonies on the soft substrates indicates that the current protocols to culture mESCs can be substantially improved by plating the mESCs on soft substrates. Furthermore, our data raise a potential significant impact of substrate stiffness on tumorigenesis by ESCs (Fig. 3.6). Understanding this role may dramatically improve the safety issue of ESCs and induced pluripotent stem cells (iPSCs) in regenerative medicine.

Recently we have shown that mESCs downregulate expression of the pluripotency marker OCT3/4 and differentiate as increased stresses via integrins are

applied externally [24]. We have recently shown that single mESCs generate low basal tractions on soft substrates and increase their basal tractions as substrate stiffness increases [38]. However, stiffness at the apical surface of single mESC does not vary with basal substrate stiffness [38]. In contrast, in this study, we show that both apical stiffness and basal tractions of mESC colonies increase with substrate stiffness, possibly due to the fact that mechanosensing capacities of the E-cadherins [39] at lateral adherens junctions have promoted mechanical interactions between the apical cytoskeleton and the basal cytoskeleton. E-cadherins have been implicated in self-renewal and pluripotency of ESCs [40, 41]. E-cadherin knockout mESCs have shown evidence of LIF independence [42]. Recently it is demonstrated that E-cadherin and myosin IIA play important roles in facilitating hESC self-renewal and survival [32]. It is possible that cell-matrix tractions and cell-cell tractions exert opposing effects on self-renewal and differentiation: high cell-matrix tractions promote differentiation whereas high cell-cell tractions promote self-renewal and pluripotency. Blebbistatin or myosin-II knockdown inhibits both cell-matrix tractions and cell-cell tractions [32]; thus the effects of these interventions on ESC pluripotency and differentiation could be complicated. We have noticed that on the same ∼8 kPa substrate, hESC colonies generate ∼10-fold higher cell-ECM tractions (RMS traction ∼600 Pa, peak traction ∼2000 Pa; ref. 32) than mESC colonies (RMS traction ∼60 Pa, peak traction ∼200 Pa; our present study), suggesting that hESC colonies may either generate much greater total force or transfer more myosin II-dependent contractility to the matrix substrate and less force between cell-cell adhesions than mESC colonies. In the future the relationship between cell-cell adhesion E-cadherins and cell-matrix adhesion in mechanics, biology, self-renewal, and pluripotency of mESCs and hESCs needs to be elucidated. The present data also show that expression of OCT3/4 is inversely associated with the traction and the stiffness of the mESC colonies. These findings lead us to the following question, what is the underlying mechanism by which soft-substrates can maintain self-renewal and pluripotency of mESCs? Our data demonstrate that mESC colonies maintain their self-renewal and pluripotency when the tractions and stiffness of the colonies are kept low on the soft substrate. In addition, pluripotency marker OCT3/4 is inversely associated with the traction and the stiffness of the mESC colonies. These data indicate that mESC colonies tend to differentiate when both myosin-II dependent

basal tractions and apical cell stiffness increase as the substrate stiffness increases. The findings of low tractions (prestress) in mESCs in the present study have been predicted from our previous analyses of molecular basis of mESC rheology using the model of molecular dynamics simulation and living cell rheological measurements [28]. Currently the exact underlying mechanism that connects the low traction and low stiffness on soft substrates with the self-renewal and pluripotency of mESCs is not clear. However, it is possible that genes essential to sustain cellular pluripotency are kept turned-on by low mechanical stresses. Once the high endogenous mechanical stresses generated on the rigid substrates are applied to the cytoskeleton and the nucleus, genes associated with cell differentiation and/or the transcription factors that regulate expression of such genes are directly activated whereas pluripotency genes are inhibited [43, 44], via the molecular mechanisms of conformational change or unfolding of cytoskeletal proteins and/or nuclear proteins [44-47]. This interpretation is consistent with a report that simulated microgravity promotes formation of ball-like ES cell colonies in the absence of LIF [48]. Alternatively, soft substrates may promote production of and/or cellular accessibility to LIF and/or other soluble growth factors to sustain self-renewal and pluripotency of mESCs. However, this alternative interpretation is not able to explain the fact that saturating amounts of LIF or other soluble growth factors alone fail to maintain homogenous populations of mESC colonies on rigid substrates, whereas soft substrates can. It is interesting that ROCK inhibitors that inhibit Rho-mediated cytoskeletal tension can promote self-renewal and pluripotency and reduce apoptosis of hESCs [49], consistent with our ideas on the role of low tractions on self-renewal and pluripotency of mESCs.

Collectively, we conclude that soft substrates promote self-renewal and pluripotency of mESCs primarily via the biophysical mechanism of low-traction/low-stiffness-dependent gene regulation. It remains to be seen if our findings and the underlying biophysical mechanism on mESCs can be extended to hESCs and iPSCs since recent advances in defining culture conditions chemically are not sufficient to prevent spontaneous differentiation of hESCs [50]. Several recent papers have reported the improved long term self-renewal of hESCs using synthetic surface molecules or recombinant matrix molecules [14-16]. However, significant challenges remains for hESC culture, since long term culture and passages of hESCs lead to significant changes of

copy number variations (CNVs) and gene expressions [51]. It is conceivable that if the substrate softness would match that of the hESCs, homogenous populations of self-renewal, pluripotent hESCs might be generated for long-term without inducing changes in CNVs and/or gene expressions.

3.5 Methods

3.5.1 Cell culture

A mouse embryonic stem cell (mESC) line, namely OGR1, that expresses EGFP under the promoter of OCT3/4 (OCT3/4::GFP) [27] was used in this study. These undifferentiated mESCs were maintained in the standard culture condition as described before (ref. 24) in the presence of Leukaemia Inhibitory Factor (LIF; Chemicon). Briefly, undifferentiated mESCs were cultured in the ES cell medium consisting of high glucose-Dulbeccos modified Eagles medium (Invitrogen) supplemented with 15% ES-qualified fetal bovine serum (FBS; Invitrogen), 2 mM L-glutamine (Invitrogen), 1mM sodium pyruvate, 0.1 mM nonessential amino acids (Invitrogen), penicillin/streptomycin, 0.1 mM beta-mercaptoethanol (Sigma), and 1000 U/ml recombinant LIF (ESGRO; Millipore) at 37°C with 5% CO_2. Cells were passaged every 2-3 days at a ratio of 1:6 using TrypLE (Invitrogen). The medium was changed daily. For experiments, cells were plated on type I collagen (Sigma)-coated (40 or 100 μg/ml) rigid dishes or type I collagen-coated (100 μg/ml) polyacrylamide gels (0.6, 3.5, and 8 kPa) and cultured up to 5 days (unless stated otherwise) with or without LIF. The polymer layer formed by the collagen-1 molecules are too thin ($\ll$0.2 μm) to affect the modulus of the polyacrylamide gel ($\sim$70 μm in thickness) that an attached cell feels. For some experiments on 8 kPa substrates we added 10 μM Blebbistatin for 5 days. Blebbistatin containing medium was changed every two days as it is stable for up to 48 hours [17].

3.5.2 Flow Cytometric Sorting

OGR1 mESCs were sorted on the i-Cyt Reflection system with a nozzle of 100 μm and at a rate of 3000 to 5000 cells/second at 20 psi. Under

the identical culture conditions, wild-type mESCs (W4, 129S6/SvEvTac) having no fluorescent protein expression were served as a negative control. Trypsinized cells were suspended in ice-cold PBS containing 10% FBS just before each experiment.

3.5.3 EB formation assay

Hanging drop cultures were prepared using 25 μl droplets each having 600 cells to initiate embryoid body (EB) formation [29]. After maintained in the presence or the absence of LIF for 3 days, mESCs were allowed to aggregate and form EBs in the bottom of the hanging drops made with the ES medium without LIF for 3 days. Then, they were transferred to adherent culture dishes. The number of EBs formed was counted and therefore the efficiency of EB formation was calculated for each test condition.

3.5.4 Teratoma formation assay

One million viable mESCs (OGR1) in ice-cold 25 μl PBS together with 25 μl of 0.3 μg/ml type-I collagen were injected into NOD-SCID mice subcutaneously. Health of mice was monitored regularly. They were humanely sacrificed after 6-7 weeks (according to the protocol approved by IACUC, University of Illinois) and teratomas were isolated. These teratomas were fixed with 4% paraformaldehyde in PBS at 4°C overnight and further processed for standard Alcian Blue, Hematoxylin and Eosin (H&E) staining.

3.5.5 Traction measurements

Cell traction measurements have been described in details elsewhere [53]. Briefly, images of red fluorescent submicrobeads (0.2μm) embedded into the apical surface of gels ($\sim$70 μm in thickness) were taken during experiments and compared with a reference image at the end of experiment after trypsinizing colonies from the substrates. The displacements of the beads were computed to generate a displacement field of the colony generating forces on the underlying substrates. A traction field was then calculated from the displacement field by an established method [54].

3.5.6 Quantification of cell stiffness

Complex stiffness was measured by applying an oscillatory magnetic field (i.e., applied specific torque, T, or the applied stress=17.2 Pa at 0.3 Hz) and measuring the resultant oscillatory bead motions (i.e., the measured strain) [24, 28, 55-57]. The stiffness has the units of torque per unit bead volume per unit bead displacement (Pa/nm), which is independent of any model. The beads were coated with saturating amounts of RGD (Arg-Gly-Asp) to bind specifically to integrin receptors. The beads were embedded ∼50% into the cell apical surface as shown earlier [24]. We used the 50% bead-cell surface contact area and an established finite element model to convert stiffness (Pa/nm) to modulus (Pa) [58] and determined that 1 Pa/nm stiffness is equivalent to 2.5 kPa modulus. In the analysis, only those beads whose displacement waves conformed to the input sinusoidal signals at the same frequency were selected which is essential to filter out the noise (e.g., spontaneous bead movements or microscope stage shifts). Beads with displacements less than 5 nm (limitation of resolution detection) and loosely bound beads were not selected for analysis. To increase signal to noise ratio, peak amplitude of the displacement d (nm) was averaged over 5 consecutive cycles.

3.5.7 Gene Expression Analysis

The same amount of total RNA (1.6 μg) from mESCs in each condition was used to synthesize the first strand cDNA as previously described [59]. PCR mixtures by Phusion DNA polymerase (NEB) were prepared according to the manufacturers instructions. The PCR conditions were as follows: first, denaturing at 98°C for 1 min, different number of cycles of denaturing at 98°C for 10 sec, annealing at 65°C for 30 sec, and extension at 72°C for 30 sec, followed by a final extension reaction at 72°C for 7.5 min. As to the PCR cycles for the samples for LIF- conditions, 16 cycles were applied for OCT3/4, ESG1 and EF1α; 25 cycles for SOX2 and TCF15; 27 cycles for TWIST2 and T(Brachyury); 29 cycles for Eras. Primer pairs used in this study have been described earlier: Eras [31], OCT3/4 [60], ESG1 and EF1α [59], TCF15 and TWIST2 [30], T [61], SOX2 [62], NANOG [63].

3.5.8 AP Staining

Mouse ESCs were fixed in Dents fixative (DMSO:100% Methanol=1:4) at -20°C for 1hr, and washed with PBS for three times. The Alkaline Phosphate (AP) kit (Sigma-Aldrich 85L3R) was used according to the manufacturers instructions.

3.5.9 Immunofluorescent microscopy

Immunofluorescent microscopy was carried out essentially as described previously [64]. Briefly, mESCs cultured on glass-bottom culture dishes (MatTek corporation) were fixed with Dents fixative at -20°C overnight, washed with PBST (0.1% Tween in PBS) twice and blocked with PBSMT (2% skimmed milk in PBST) for 1hr. Fixed mESCs were incubated with goat anti-mouse NANOG polyclonal antibody (R&D systems) diluted with PBMST at the 1:200 ratio at 4°C overnight. Normal lamb serum was diluted with PBSMT at 1:1,000 and used as a negative control. After two washes with PBSMT for 30min each at 4°C followed by three more washes at room temperature, Alexa Fluor 546 rabbit anti-goat IgG (Molecular Probes) was diluted with PBSMT at the 1:400 ratio and used as a secondary antibody. After five washes with PBSMT as before, stained mESCs were incubated with DAPI (5 μg/ml, Sigma) at room temperature for 15 min, and mounted into glycerol gelatin (Sigma) for fluorescence microscopy (Leica DMI4000B).

Immunofluorescent microscopy for paraffin-embedded sections of teratomas was carried out as described already [64] with following modifications. Deparaffinized 4-6 μm sections were rehydrated with Histo-clear II (Fisher)-alcohol series, immersed in 10 mM sodium citrate buffer (pH 6.0) [65], and heated by a microwave oven (LG, 1200W) for 5 min at level 5, 3 times. Then, blocked sections were incubated at RT for 1.5 hr with culture supernatant from mouse anti-nestin monoclonal antibody (Rat-401 raised by Dr. Susan Hockfield), or goat anti-a-fetoprotein (Santa Cruz Biotechnology Inc.) or rabbit anti-a-smooth muscle actin polyclonal antibodies (Abcam) diluted with 2% skimmed milk in PBS with 0.1% Tween 20 (PBSMT) at 1:100. Normal mouse, rabbit, or lamb sera diluted with PBSMT at 1:250 were used as negative controls. After 3 washes with PBSMT at RT for 10 min each, sections were incubated at RT for 1.5 hr with Alexa Fluor 488-conjugated goat

anti-mouse IgG (whole molecule; Invitrogen), or Alexa Fluor 546-conjugated rabbit anti-goat or goat anti-rabbit IgG (whole molecule; Invitrogen) diluted with PBSMT at 1:400. After 4 washes with PBSMT, sections were stained with 0.5mg/ml DAPI (Sigma) in PBS, and mounted with glycerol-gelatin (Sigma).

3.5.10 Serial Passaging on soft substrates

An undifferentiated mESC line, W4 (129/SvEv), was serially passaged on rigid dish and soft gel (0.6 kPa) under LIF +/- condition for over three months. Both rigid dish and soft gel were coated with type I collagen. W4 cells were thawed on mitotically inactivated primary mouse embryonic fibroblast. After recovery, W4 cells were passaged onto 0.1% gelatin coated polystyrene tissue culture dishes couple of times to remove feeders. Then W4 cells were plated on rigid dishes or soft gels. On soft gels, cells were initially plated at a high concentration which was found to be useful particularly for LIF- condition. On the very first passage, cells were first plated with LIF+ medium. LIF+ medium was withdrawn the following day from one of the soft gels and labeled as LIF- condition. From this point onward exogenous LIF was never added for the LIF- condition on the subsequent passages. W4 cells on gel were passaged 1:3 ratio on subsequent passages. The medium was changed every two days and passaged every 3-4 days.

3.5.11 Polyacrylamide Substrates

Polyacrylamide substrates were made of as described before [66]. The elastic Youngs modulus of the polyacrylamide substrates used in this study was 0.6 kPa (0.06% bis-acrylamide,3%polyacrylamide), 3.5 kPa (0.1% bis-acrylamide, 5% polyacrylamide), and 8 kPa (0.3% bis-acrylamide, 5% polyacrylamide) [67, 68)] Red fluorescent microspheres (0.2 μm; Molecular Probe) were embedded onto the gels for traction measurements so that EGFP expression in OGR1 mESC colonies did not interfere with traction measurements.

3.5.12 Statistical Analysis

Students t-test was applied to all statistical analyses.

3.6 References

[1] Hayashi, K., C. de Sousa, S.M. Lopes, F. Tang, and M.A. Surani, "Dynamic equilibrium and heterogeneity of mouse pluripotent stem cells with distinct functional and epigenetic states". *Cell Stem Cells* 3, pp.391-401, 2008.

[2] Chambers, I. et al., "Nanog safeguards pluripotency and mediates germline development". *Nature* 450, pp.1230-1234, 2007.

[3] Singh, A.M., T. Hamazaki, K.E. Hankowski, and N. Terada, "A heterogeneous expression pattern for Nanog in embryonic stem cells". *Stem Cells* 25, pp.2534-2542, 2007.

[4] Furusawa, T. et al., "Gene expression profiling of mouse embryonic stem cell subpopulations". *Biol. Reprod.* 75, pp.555-561, 2006.

[5] Toyooka, Y., D. Shimosato, K. Murakami, K. Takahashi, and H. Niwa, "Identification and characterization of subpopulations in undifferentiated ES cell culture". *Development* 135, pp.909-918, 2008.

[6] Suzuki, A. et al., "Nanog binds to Smad1 and blocks bone morphogenetic protein-induced differentiation of embryonic stem cells". *Proc. Natl. Acad. Sci. USA* 103, pp.10294-10299, 2006.

[7] Carter, M.G. et al., "An in situ hybridization-based screen for heterogeneously expressed genes in mouse ES cells". *Gene Expr Patterns* 8, pp.181-198, 2008.

[8] Tanaka, T.S., "Transcriptional heterogeneity in mouse embryonic stem cells". *Reprod Fertil Dev.* 21, pp.67-75, 2009.

[9] Zalzman, M. et al., "Zscan4 regulates telomere elongation and genomic stability in ES cells". *Nature* 464, pp.858-863, 2010.

[10] Hayashi, K., S.M. Lopes, F. Tang, and M.A. Surani, "Dynamic equilibrium and heterogeneity of mouse pluripotent stem cells with distinct functional and epigenetic states". *Cell Stem Cell* 3, pp.391-401, 2008.

[11] Ying, Q.L., J. Nichols, I. Chambers, and A. Smith, "BMP induction of Id proteins suppresses differentiation and sustains embryonic stem cell self-renewal in collaboration with STAT3". *Cell* 115, pp.281-292, 2003.

[12] Ying, Q. L. et al., "The ground state of embryonic stem cell self-renewal". *Nature* 453, pp.519-523, 2008.

[13] Furue, M. et al., "Leukemia inhibitory factor as an anti-apoptotic mitogen for pluripotent mouse embryonic stem cells in a serum-free medium without feeder cells". *In Vitro Cell Dev Biol Anim* 41, pp.19-28, 2005.

[14] Melkoumian, Z. et al., "Synthetic peptide-acrylate surfaces for long-term self-renewal and cardiomyocyte differentiation of human embryonic stem cells". *Nat Biotechnol* 28, pp.606-610, 2010.

[15] Rodin, S. et al., "Long-term self-renewal of human pluripotent stem cells on human recombinant laminin-511". *Nat Biotechnol* 28, pp.611-615, 2010.

[16] Villa-Diaz, L.G. et al., "Synthetic polymer coatings for long-term growth of human embryonic stem cells". *Nat Biotechnol.* 28, pp.581-583, 2010.

[17] Engler, A.J., S. Sen, H.L. Sweeney, and D.E. Discher, "Matrix elasticity directs stem cell lineage specification". *Cell* 126, pp.677-689, 2006.

[18] Discher, D.E., P. Janmey, and Y.L. Wang, "Tissue cells feel and respond to the stiffness of their substrate". *Science* 310, pp.1139-1143, 2005.

[19] Vogel, V. and M.P. Sheetz, "Local force and geometry sensing regulate cell functions". *Nature Rev Mol Cell Biol* 7, pp.265-275, 2006.

[20] Saha, K. et al., "Substrate modulus directs neural stem cell behavior". *Biophys J* 95, pp.4426-4438, 2008.

[21] Evans, N.D. et al., "Substrate stiffness affects early differentiation events in embryonic stem cells". *Eur Cell Mater* 18, 1-14, 2009.

[22] Lutolf, M.P., P.M. Gilbert, and H.M. Blau, "Designing materials to direct stem-cell fate". *Nature* 462, 433-441, 2009.

[23] Discher, D.E., D.J. Mooney, and P.W. Zandstra, "Growth factors, matrices, and forces combine and control stem cells". *Science* 324, pp.1673-1677, 2009.

[24] Chowdhury, F. et al., "Material properties of the cell dictate stress-induced spreading and differentiation in embryonic stem cells". *Nature Mater* 9, pp.82-88, 2010.

[25] Feinberg, A.W., L.C. Zhao, and A.B. Brennan, "Quantifying Inter-Cellular Forces in Bioadhesion: Examination of Sialyl Lewis X and Selectin Interactions with Atomic Force Microscopy". *25th Annual Meeting of The Adhesion Society* Orlando, FL, 2002.

[26] Hayashi, Y. et al., "Integrins regulate mouse embryonic stem cell self-renewal". *Stem Cells* 25, pp.3005-3015 (2007).

[27] Walker, E. et al., "Prediction and Testing of Novel Transcriptional Networks Regulating Embryonic Stem Cell Self-Renewal and Commitment". *Cell Stem Cell* 1, pp.71-86, 2007.

[28] Chowdhury, F. et al., "Is cell rheology governed by nonequilibrium-to-equilibrium transition of noncovalent bonds"? *Biophys J* 95, pp.57195727, 2008.

[29] Zandstra, P.W., H.V. Le, G.Q. Daley, L.G. Griffith, and D.A. Lauffenburger, "Leukemia inhibitory factor (LIF) concentration modulates embryonic stem cell self-renewal and differentiation independently of proliferation". *Biotechnol Bioeng* 69, pp.607-617, 2000.

[30] Tanaka, T.S., R.E. Davey, Lan, Q., P.W. Zandstra, and W.L. Stanford, "Development of a gene-trap vector with a highly sensitive fluorescent protein reporter system for expression profiling". *Genesis* 46, pp.347-356, 2008.

[31] Takahashi, K., K. Mitsui, and S. Yamanaka, "Role of ERas in promoting tumour-like properties in mouse embryonic stem cells". *Nature* 423, pp.541-545, 2003.

[32] Li, D. et al., "Integrated biochemical and mechanical signals regulate multifaceted human embryonic stem cell functions". *J Cell Biol.* 191, pp.631-44, 2010.

[33] Tullio, A. N. et al., "Nonmuscle myosin II-B is required for normal development of the mouse heart". *Proc Natl Acad Sci USA* 94, pp.12407-12412, 1997.

[34] Conti, M.A., S. Even-Ram, C. Liu, K.M. Yamada, and R.S. Adelstein, "Defects in cell adhesion and the visceral endoderm following ablation of nonmuscle myosin heavy chain II-A in mice". *J Biol Chem* 279, pp.41263-41266, 2004.

[35] Engler AJ, et al., "Embryonic cardiomyocytes beat best on a matrix with heart-like elasticity: scar-like rigidity inhibits beating". *J Cell Sci.* 121, pp.794-802, 2008.

[36] Engler, A. J. et al., "Myotubes differentiate optimally on substrates with tissue-like stiffness: pathological implications for soft or stiff microenvironments". *J Cell Biol.* 166, pp.877-87, 2004.

[37] Gilbert, P.M. et al., "Substrate elasticity regulates skeletal muscle stem cell self-renewal in culture". *Science* 329(5995), pp.1078-81, 2010.

[38] Poh, Y.C., F. Chowdhury, T.S. Tanaka, and N. Wang, "Embryonic stem cells do not stiffen on rigid substrates". *Biophys J* 99, pp.L19-21, 2010.

[39] le Duc, Q. et al., "Vinculin potentiates E-cadherin mechanosensing and is recruited to actin-anchored sites within adherens junctions in a MyosinII dependent manner". *J Cell Biol* 189, pp.1107-1115, 2010.

[40] Xu, Y. et al., "Revealing a core signaling regulatory mechanism for pluripotent stem cell survival and self-renewal by small molecules". *Proc Natl Acad Sci USA* 107, pp.8129-8134, 2010.

[41] Nagaoka, M., K. Si-Tayeb, T. Akaike, and S.A. Duncan, "Culture of human pluripotent stem cells using completely defined conditions on a recombinant E-cadherin substratum". *BMC Dev Biol* 10, pp.60, 2010.

[42] Soncin, F. et al., "Abrogation of E-cadherin-mediated cell-cell contact in mouse embryonic stem cells results in reversible LIF-independent self-renewal". *Stem Cells* 27, pp.2069-2080, 2009.

[43] Wang, N., J.D. Tytell, and D.E. Ingber, "Mechanotransduction at a distance: mechanically coupling the extracellular matrix with the nucleus". *Nat Rev Mol Cell Biol* 10, pp.75-82, 2009.

[44] Na, S. et al., "Rapid signal transduction in living cells is a unique feature of mechanotransduction". *Proc Natl Acad Sci USA* 105, pp.6626-6631, 2008.

[45] Brown, A.E. and D.E. Discher, "Conformational changes and signaling in cell and matrix physics". *Curr Biol* 19, pp.R781-789, 2009.

[46] del Rio, A. et al., "Stretching single talin rod molecules activates vinculin binding". *Science* 323, pp.638-641, 2009.

[47] Johnson, C.P., H.Y. Tang, C. Carag, D.W. Speicher, and D.E. Discher, "Forced unfolding of proteins within cells". *Science* 317, pp.663-666, 2007.

[48] Kawahara, Y. et al., "LIF-free embryonic stem cell culture in simulated microgravity". *PLoS ONE* 4, pp.e6343, 2009.

[49] Watanabe, K. et al., "A ROCK inhibitor permits survival of dissociated human embryonic stem cells". *Nat. Biotechnol* 25, pp.681686, 2007.

[50] Ludwig, T. E. et al., "Derivation of human embryonic stem cells in defined conditions". *Nat Biotechnol* 24, pp.185-187, 2006.

[51] Närvä, E. et al., "High-resolution DNA analysis of human embryonic stem cell lines reveals culture-induced copy number changes and loss of heterozygosity". *Nat Biotechnol* 28, pp.371-377, 2010.

[52] Duval, D., B. Reinhardt, C. Kedinger, and H. Boeuf, "Role of suppressors of cytokine signaling (Socs) in leukemia inhibitory factor (LIF) -dependent embryonic stem cell survival". *FASEB J* 14, pp.1577-1584, 2000.

[53] Wang, N. et al., "Cell prestress I. Stiffness and prestress are closely associated in adherent contractile cells". *Am J Physiol Cell Physiol* 282, pp.C606-616, 2002.

[54] Butler, J.P., I.M. Toli-Nrrelykke, Fabry, B. and J.J. Fredberg, "Traction fields, moments, and strain energy that cells exert on their surroundings". *Am J Physiol Cell Physiol* 282, pp.C595-605, 2002.

[55] Wang, N., J.P. Butler, and D.E. Ingber, "Mechanotransduction across the cell surface and through the cytoskeleton". *Science* 260, pp.11241127, 1993.

[56] Trepat, X. et al., "Universal physical responses to stretch in the living cell". *Nature* 447, pp.592595, 2007.

[57] Bursac, P. et al., "Cytoskeletal remodelling and slow dynamics in the living cell". *Nature Mater* 4, pp.557561, 2005.

[58] Mijailovich, S.M., M. Kojic, M. Zivkovic, B. Fabry, and J.J. Fredberg, "A finite element model of cell deformation during magnetic bead twisting". *J Appl Physiol* 93, pp.1429-1436, 2002.

[59] Tanaka, T. S. et al., "Gene expression profiling of embryo-derived stem cells reveals candidate genes associated with pluripotency and lineage specificity". *Genome Res* 12, pp.1921-1928, 2002.

[60] Nichols, J. et al., "Formation of Pluripotent Stem Cells in the Mammalian Embryo Depends on the POU Transcription Factor Oct". *Cell* 95, pp.379-91, 1998.

[61] Fujikura, J. et al., "Differentiation of embryonic stem cells is induced by GATA factors". *Genes Dev.* 16, pp.784-789, 2002.

[62] Masui, S. et al., "Pluripotency governed by Sox2 via regulation of Oct3/4 expression in mouse embryonic stem cells". *Nat. Cell Biol.* 9, pp.625-635, 2007.

[63] Mitsui, K. et al., "The homeoprotein Nanog is required for maintenance of pluripotency in mouse epiblast and ES cells". *Cell* 113, pp.631-642, 2003.

[64] Tanaka, T. S. et al., "Esg1, expressed exclusively in preimplantation embryos, germline, and embryonic stem cells, is a putative RNA-binding protein with broad RNA targets". *Dev. Growth Differ.* 48, pp.381390, 2006.

[65] Lan, H.Y., W. Mu, D.J. Nikolic-Paterson, and R.C. Atkins, "A novel, simple, reliable, and sensitive method for multiple immunoenzyme staining: Use of microwave oven heating to block antibody crossreactivity and retrieve antigens". *J. Histochem. Cytochem.* 43, pp.97-102, 1995.

[66] Pelham, R.J. Jr. and Y. Wang, "Cell locomotion and focal adhesions are regulated by substrate flexibility". *Proc. Natl. Acad. Sci. USA* 94, pp.13661-13665, 1997.

[67] Yeung, T. et al., "Effects of substrate stiffness on cell morphology, cytoskeletal structure, and adhesion". *Cell Motil Cytoskeleton* 60, pp.24-34, 2005.

[68] Engler, A. et al., "Substrate compliance versus ligand density in cell on gel responses". *Biophys J* 86, pp.617-628, 2004.

Figure 3.1: Soft substrates promote mouse embryonic stem cell (mESC) self-renewal

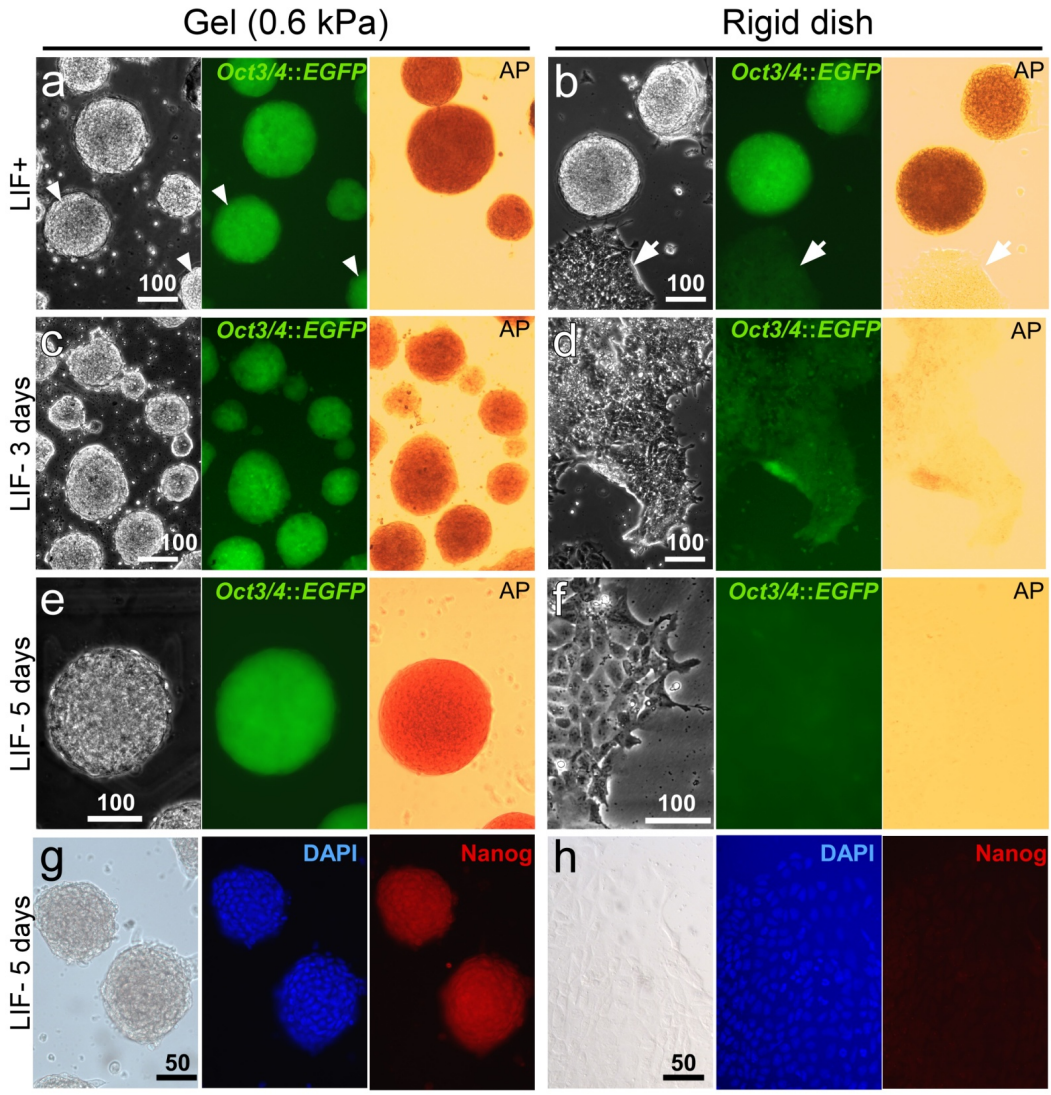

a, *mESCs on the substrates of 0.6 kPa stiffness (Gel (0.6 kPa)) always formed round and compact colonies (left) with uniform OCT3/4::GFP expression (middle) and the high AP activity (right) in the presence of LIF (LIF+). Arrowheads indicate that marked colonies were washed out during the staining procedure to measure the AP activity.* **b**, *mESCs on the rigid substrates of polystyrene dishes (Rigid dish) with LIF formed round colonies and a spread irregular colony (left; white arrows) with heterogeneous OCT3/4::GFP expression (middle) and varying degrees of the AP activity (right).* **c**, *mESCs on the soft substrates without LIF for 3 days (LIF- 3 days) still formed round colonies with uniform OCT3/4::GFP expression and the AP activity maintained.* **d**, *mESCs on the rigid dish without LIF for 3 days exhibited irregular*

spread colonies with OCT3/4::GFP expression and the AP activity reduced dramatically. **e**, *The soft substrates supported mESC self-renewal without LIF for 5 days (LIF- 5days) with high uniform OCT3/4::GFP expression and the AP activity maintained.* **f**, *On the rigid dishes, 5 days of culture without LIF resulted in irregular spread colonies with extremely low OCT3/4::GFP expression and a undetectable AP activity.*($\mathbf{g} - \mathbf{h}$), *Immunocytochemistry with mESCs maintained on the soft (g) or the rigid substrates (h) without LIF for 5 days. Images for bright field (left) and nuclear staining with DAPI (middle) show appearance of colonies. High NANOG expression was observed in the mESCs on the soft substrates (g, right), but not in the ones on the rigid dish (h, right). Three independent experiments showed very similar results. Bars, 100 (a-f) or 50 (g & h) μms.[Chowdhury et al. (2010) PLoS ONE 5(12): e15655]*

Figure 3.2: Mouse ESCs were plated on collagen-1 (100 μg/ml) coated rigid dishes

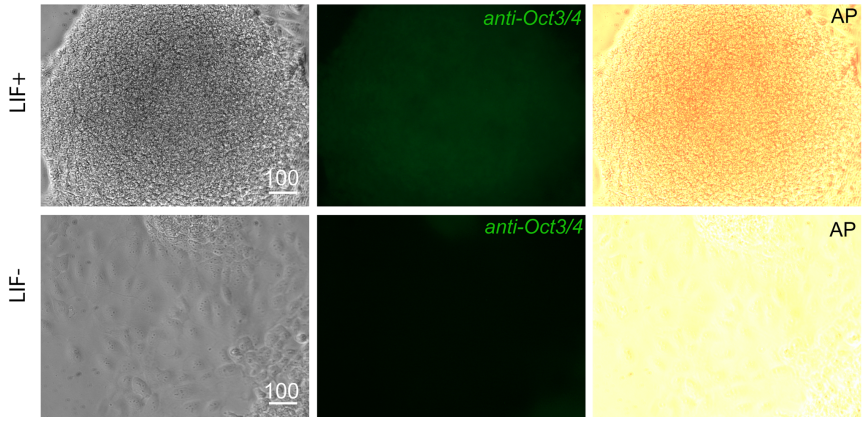

Mouse ESCs were plated on collagen-1 (100 μg/ml) coated rigid dishes and cultured for 5 days in LIF+/- conditions. The colonies were immunostained for OCT3/4 and the alkaline phosphatase (AP) activity. Colonies exhibited similar phenotypes to the ones maintained on 40 μg/ml collagen-1. [Chowdhury et al. (2010) PLoS ONE 5(12): e15655]

Figure 3.3: Mouse embryonic stem cells (mESCs; OGR1) thawed and maintained on soft gels formed round and compact colonies as they did on feeders

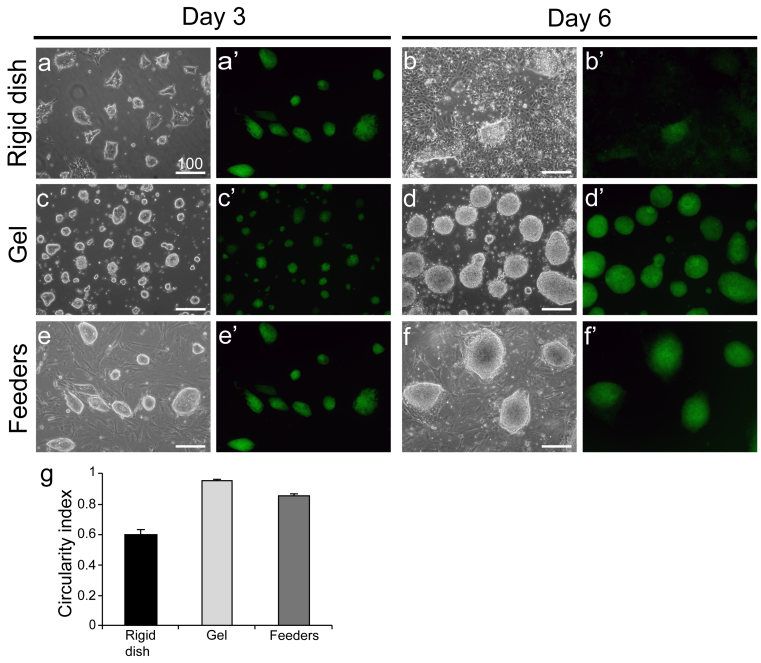

Bright $(\mathbf{a}-\mathbf{f})$ *and dark* $(\mathbf{a}'-\mathbf{f}')$ *field images are shown.* $(\mathbf{a}-\mathbf{a}')$ *ORG1 mESCs thawed on rigid dishes formed small spread colonies on day 3. However, OCT3/4::GFP expression at this stage were not significantly diminished.* $(\mathbf{b}-\mathbf{b}')$ *mESCs thawed on rigid dishes on day 6 showed appearance of spread and differentiated cells. The corresponding dark field image showed very low GFP expression.* $(\mathbf{c}-\mathbf{c}')$ *mESCs thawed on the soft gels started to form round and compact colony on day 3 with GFP expression.* $(\mathbf{d}-\mathbf{d}')$ *on day 6, these mESCs on the soft gel still formed very round and compact colonies with GFP uniformly expressed.* $(\mathbf{e}-\mathbf{e}')$ *On day 3, mESCs thawed on feeders appeared to have colonies of various shapes ranging from relatively round to somewhat flattened (white arrow in* $\mathbf{e}$*). The flattened colony showed low GFP expression (arrow in* $\mathbf{e}$*).* $(\mathbf{f}-\mathbf{f}')$ *On day 6, mESCs formed relatively round colonies on feeders with GFP expression, except for the cells on the edge of the colony whose GFP expression was relatively low, showing early signs of differentiation.* $\mathbf{g}$*, Comparisons among the shapes of colonies on the rigid dish, the gel and the feeders by quantifying the colony shape factor [68]. The colony shape factor (=*4π *Area/Perimeter*^{2}*; Area=colony projected area; Perimeter=perimeter length of a colony) measures to what extent the colony is similar to a true circle. A true circle has a value of unity. Data are mean s.e.m., n=29, 32, 30 colonies for the rigid dish, the gel and the feeders respectively.* $p<0.0001$ *between any two conditions. Bars, 100* μ*m. [Chowdhury et al. (2010) PLoS ONE 5(12): e15655]*

Figure 3.4: Quantification of OCT3/4 expression mESCs on soft substrates or rigid substrates

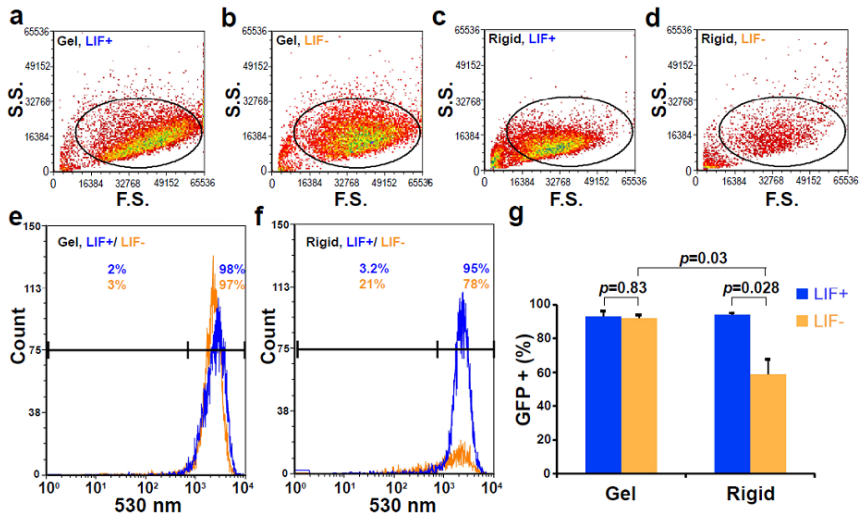

(**a** – **d**) *Representative density plots for FACS (fluorescence-activated cell sorting) of mESCs in each condition are shown. The x-axis is for forward scatter and the y-axis, side scatter. An identical gate was applied to all conditions. LIF- condition on rigid dishes yields less number of cells as some cells lose adhesion and float away [52]. This can be seen in the density plot in* (**d**). **e**, *Representative plots showing high OCT3/4::GFP expression (530 nm) found in cells maintained in the presence (blue) or absence (orange) of LIF. The threshold of GFP expression is arbitrarily determined according to the result from sorting wild-type mESCs (W4) that do not express any fluorescent protein. Two or three percentages of sorted mESCs on the soft substrates with or without LIF are GFP-negative, respectively.* **f**, *The percentage of GFP-negative mESCs increased to 21% of sorted mESCs on the rigid substrates without LIF from 3.2% of those with LIF.* **g**, *Data summary shows OCT3/4::GFP-positive mESCs on the soft substrates or the rigid substrates with or without LIF. An identical gate was applied to all replicates. Mean ± s.e. (n=4); at least three independent experiments. [Chowdhury et al. (2010) PLoS ONE 5(12): e15655]*

Figure 3.5: Functional validation and transcript analysis of mESCs on soft substrates

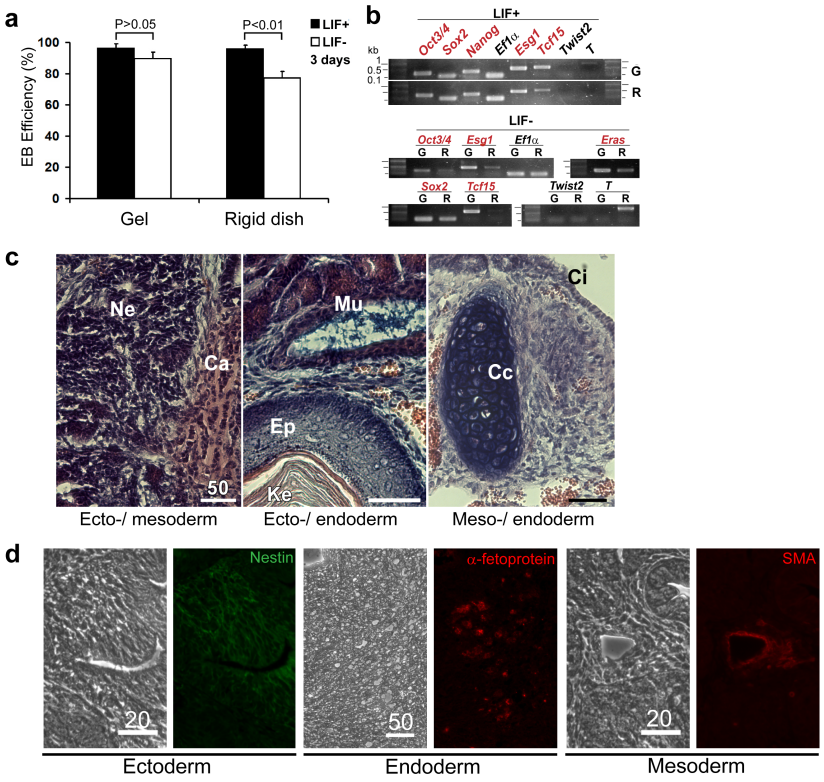

a, *Efficiencies of embryoid body (EB) formation are compared among of mESCs cultured on soft substrates and rigid dishes with or without LIF. mESCs on soft substrate retain higher EB forming capacity even in the absence of LIF as compared to those on rigid dishes.* **b** *Semi-quantitative RT-PCR was carried out with cDNAs from mESCs cultured in LIF+ and LIF- medium for 5 days either on the soft substrates (G) or the rigid substrates (R). Expression of pluripotency markers OCT3/4, ESG1, SOX2 and TCF15, the pan-mesodermal maker Brachyury (T), the late mesodermal maker TWIST2, and the tumorigenic marker ERAS were analyzed. EF1α is a loading control. Duplicates showed similar results.* **c**, *mESCs cultured on soft substrates without LIF for 5 days developed a teratoma, when injected into NOD-SCID mice subcutaneously, giving rise to all three germ layers. Ne, neural tissue; Ca, cartilage; Mu, Mucous membrane; Ep, epidermis; Ke, keratin pearl; Cc, chondroitin sulfate-rich cartilage; Ci, ciliated epithelium. Bars, 50 μm.* **d**, *mESCs cultured on soft substrates with LIF for 5 days developed a teratoma. The paraffin-embedded teratoma sections confirmed the presence of all three germ layers by immunostaining (nestin: ectoderm, α-fetoprotein: endoderm, and α-smooth muscle actin: mesoderm). Bars, 20 and 50 μm as indicated. [Chowdhury et al. (2010) PLoS ONE 5(12): e15655]*

Figure 3.6: Mouse ESCs maintained on soft gels under LIF+ and LIF- conditions formed a well-developed teratoma when transplanted into NOD-SCID mice subcutaneously

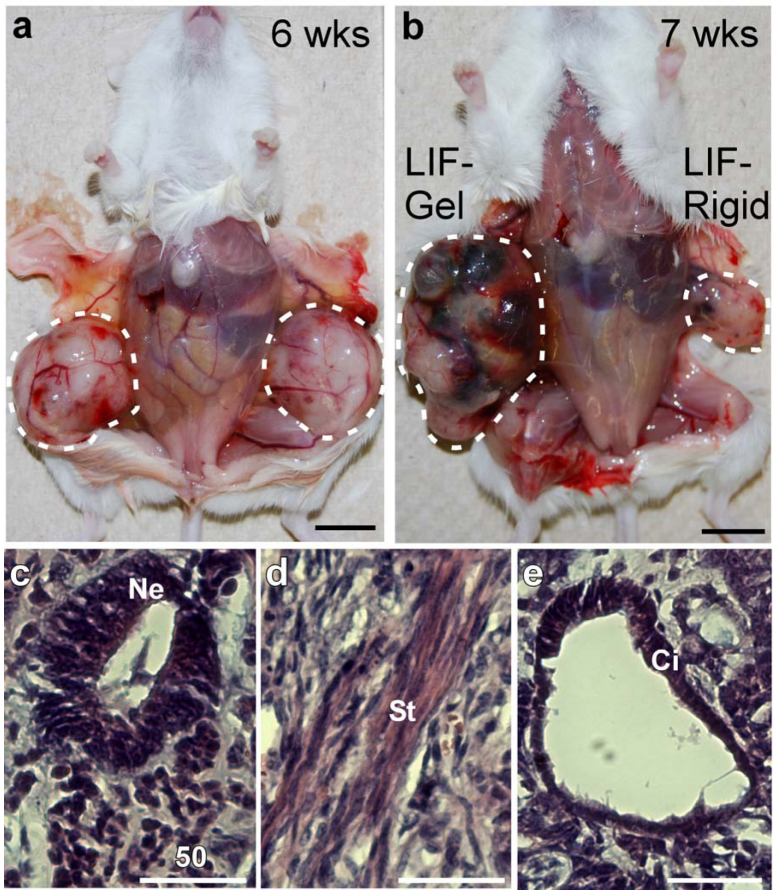

a, *Teratomas (dashed circles) are developed from mESCs cultured on the soft gel in the presence of LIF.* **b**, *The teratoma on left is developed from mESCs on the soft gel, whereas the teratoma on right is from ones on rigid dishes in the absence of LIF. n=2 separate mice. The teratoma on right is significantly smaller in size.* $(\mathbf{c}-\mathbf{e})$ *Hematoxylin and Eosin (H & E) staining of sections from a teratoma of mESCs maintained on the soft gel with LIF shows the presence of cells from all three germ layers. Ne: Neural tissue (ectoderm); St: Striated muscle (mesoderm); Ci: Ciliated epithelium (endoderm). [Chowdhury et al. (2010) PLoS ONE 5(12): e15655]*

Figure 3.7: Undifferentiated mouse ES cell line, W4 (129/SvEv), was serially passaged (images shown at passage 15) on rigid dishes and soft gels (0.6 kPa) under LIF +/- conditions for over three months

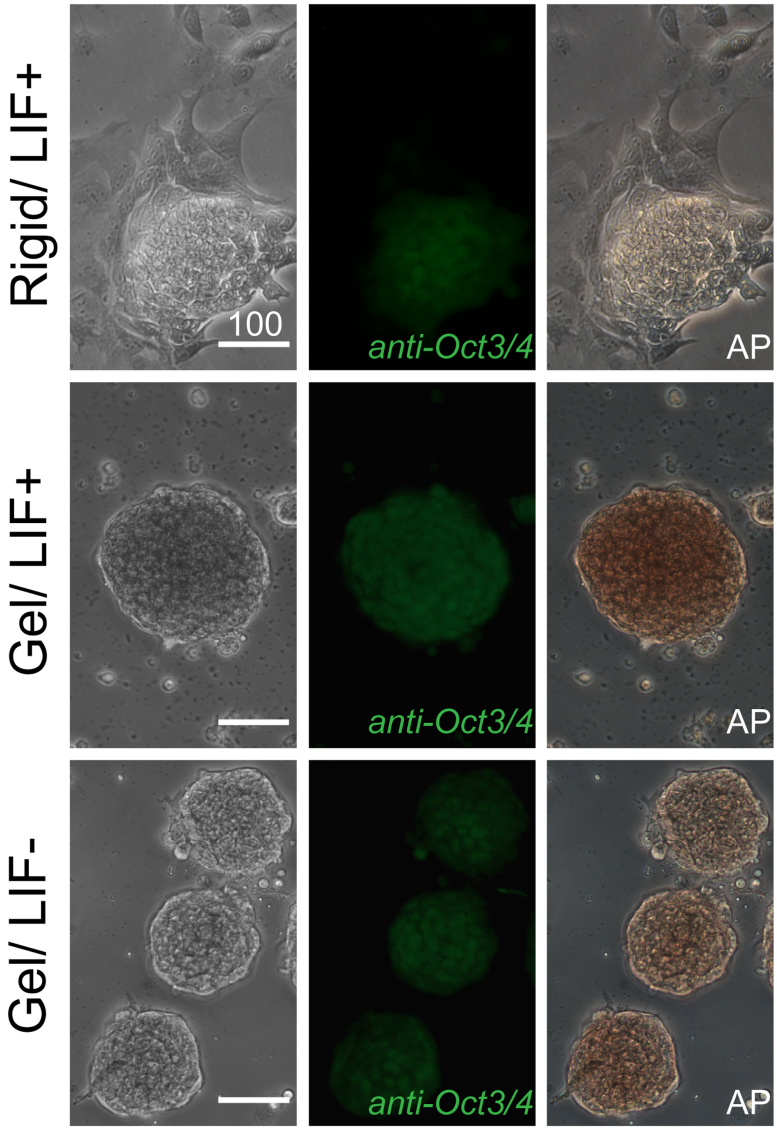

Even in the presence of LIF on rigid dishes, cells start to exhibit decreased OCT3/4 expression and the AP activity accompanied by appearance of differentiated cells at the colony periphery (row 1). However, their self-renewal was maintained best on soft gels in the presence of LIF, evident by the high OCT3/4 expression level, the high AP activity, and compact and round morphology (row 2). Remarkably, cells on soft gels also maintained self-renewal in the absence of LIF with sustained OCT3/4 expression and the AP activity (row 3). [Chowdhury et al. (2010) PLoS ONE 5(12): e15655]

Figure 3.8: Elevated endogenous stress and stiffness lead to mESC differentiation

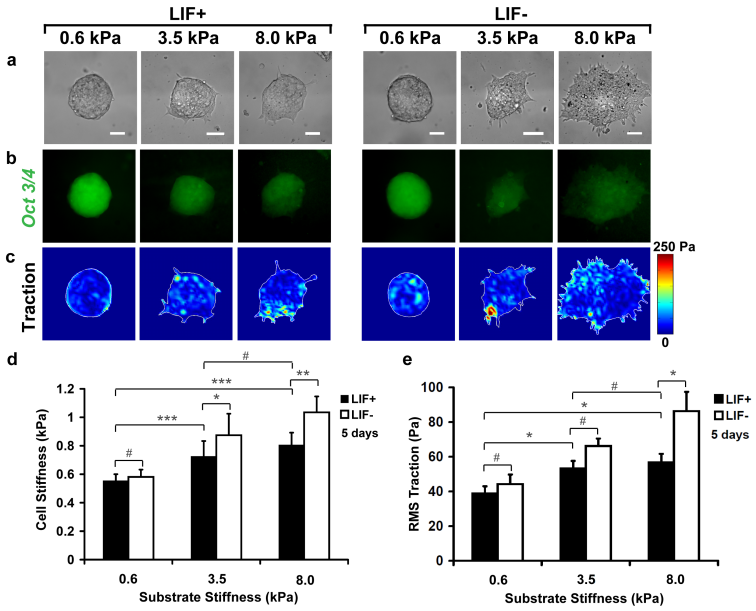

a, *Bright-field images of colonies on 0.6, 3.5 or 8 kPa substrates with or without LIF. Colonies are round and compact on 0.6 kPa substrates in the presence and absence of LIF. In contrast, colonies on 3.5 kPa, similar to 8 kPa substrates, are spread in the presence of LIF and even more spread and irregular in the absence of LIF.* **b**, *Corresponding GFP images of OCT3/4 expression of the same colonies on 0.6, 3.5 or 8 kPa substrates. Uniform OCT3/4::GFP expression is found in colonies on 0.6 kPa substrates but not on 3.5 and 8 kPa substrates.* **c**, *Colonies on 0.6 kPa substrates exert lower tractions than colonies on 3.5 and 8 kPa substrates.* **d**, *Summarized data shows that stiffnesses of the colonies are significantly different between 0.6 and 3.5 kPa substrates, and between 0.6 and 8 kPa substrates, but similar between 3.5 and 8 kPa (all are in LIF+ conditions). Colony stiffnesses are similar with (n=52) or without (n=50) LIF on 0.6 kPa substrates, but are significantly different between with (n=22) or without (n=19) LIF on 3.5 kPa, and on 8 kPa substrates (n= 85, 10 colonies with or without LIF). Mean ± s.e.* **e**, *RMS (root-mean-square) tractions of colonies on 0.6, 3.5 or 8 kPa substrates. In the presence of LIF, when substrate stiffness increased from 0.6 kPa to 3.5 kPa or to 8 kPa, tractions significantly increased. Tractions on 0.6 kPa were similar with (n=8) or without (n=7) LIF; tractions on 3.5 kPa were also similar with (n=7) or without (n=6) LIF, but tractions on 8 kPa substrates were different with (n=6) or without (n=7) LIF. Mean ± s.e. Bars, 50 μm. (*, p<0.05; **, p<0.01; ***, p<0.001; #, p>0.05) [Chowdhury et al. (2010) PLoS ONE 5(12): e15655]*

Figure 3.9: Blebbistatin (10 μM) treatment on 8 kPa substrates for 5 days decreases RMS tractions

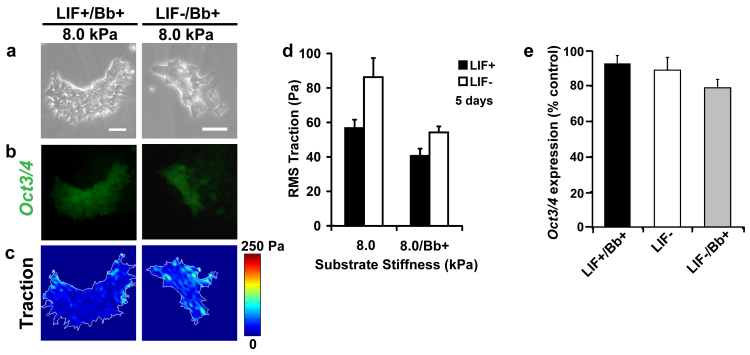

(**a** − **c**) *Blebbistatin treatment altered colony shape* (**a**)*, OCT3/4 expression* (**b**)*, and tractions* (**c**)*.* **d***, For LIF+ conditions, adding blebbistatin down-regulated tractions (p=0.032; n=10 colonies). Similary, for LIF- conditions, addition of blebbistatin decreased tractions (p=0.03; n= 8 colonies). Mean* ± *s.e.m. Bars, 50 µm.* **e***, Summarized data for OCT3/4 expression after blebbistatin treatment. Control: colonies on 8 kPa with LIF (n=9). Blebbistatin significantly lowered the level of OCT3/4 expression in colonies without LIF (n=6) when compared with the control (p<0.01). LIF withdrawal alone (n=7) or blebbistatin added to LIF+ condition (n=8) decreased OCT3/4 expression from the control only slightly but not significantly (p>0.25). Mean* ± *s.e. [Chowdhury et al. (2010) PLoS ONE 5(12): e15655]*

CHAPTER 4

CONCLUSIONS AND FUTURE DIRECTIONS

4.1 Summary

The central theme of this dissertation was to determine the effect of physical and mechanical cues on embryonic stem cells. We discovered a significant role of local cyclic stresses or underlying substrates in cell fate decisions of embryonic stem cells. In one hand, this dissertation illustrates a novel mechanism of how to differentiate ESCs and on the other hand it demonstrates how to keep them in an undifferentiated state solely by manipulating mechanical factors. The work presented in Chapter 2 identifies a novel mechanism of embryonic stem cell differentiation. It is the cell material property- cell softness of ESCs that leads to a higher strain (for a given stress) than other stiffer differentiated cell types and finally when reached a threshold strain ESCs commit to differentiate. Conversely, when ESCs experience less forces simply via down-regulation of cell-matrix tractions by culturing them on soft substrates as opposed to rigid polystyrene dishes we observed a homogeneous self renewal and maintenance of pluripotency as depicted in Chapter 3.

The idea of stress-mediated gene expression is not novel. Some of these earlier studies were generally carried out by stretching or shearing by fluid flow over entire cell surfaces followed by analyses which include average gene expression changes from several million cells. Thus, it is difficult to reveal underlying biophysical mechanisms of mechanotransduction. The work presented in Chapter 2 reveals for the first time that a small cyclic stress via focal adhesions can downregulate OCT3/4 gene expression in normal intact embryonic stem cells due to the soft material property of the cells. It is showed in Chapter 2 that intracellular softness can determine cellular sensitivity to force at a given substrate stiffness. We fixed the substrate stiffness (to 0.6 kPa) and the soluble factor (e.g. the ES cell culture medium). Then

we applied a small cyclic local stress to either soft ESCs or stiff ESD cells. We found a strong positive correlation between ESC softness and cell spreading and subsequent OCT3/4 downregulation in response to the cyclic loading.

To recapitulate the biophysical mechanism that addresses how ESCs respond biologically to locally applied stresses we see that it is the cell material property- cell softness of ESCs which makes them very sensitive to a locally applied stresses. Since ESCs are intrinsically soft, for a given applied stress level, the resulting strain is much higher than other stiffer differentiated cell types. Therefore the deformation of the cytoskeleton and its associated proteins is also higher in ESCs which in turn dictates stress-triggered spreading and differentiation of embryonic stem cells. The work presented in this Chapter 2 provides a functional significance to the recent findings on forced unfolding of proteins [1, 2] and signaling molecules [3] within cells. Thus we see that ESCs can be differentiated simply based on external mechanical forces. Perhaps, the work presented in Chapter 2 is best described by Fig. 4.1 [4].

In Chapter 3 we addressed a long-standing problem in the field of stem cell biology to keep ESCs in an undifferentiated state of growth by manipulating their local microenvironment. ESCs are adapted to in vitro culture condition by plating them on rigid plastic dishes which is million times [5] stiffer than their intrinsic stiffness. Consequently, the ESCs respond to the substrate stiffness by fluctuating expression of pluripotent genes and sporadic expression of differentiated genes and the culture results in a heterogeneous cell population. This also hinders the induction of differentiation processes as precursor materials (ESCs) are non-homogeneous. Therefore, we hypothesized that culturing them on a substrate with similar stiffness as their intrinsic stiffness would be the key to this problem. Importantly, we showed the mechanism by which our novel method can keep these ESCs in an unlimited self-renewal state. This is solely due to the downregulation of cell-matrix traction generated by these cells. When we started to elevate cell-matrix tractions, the ESCs began to lose self-renewal and pluripotency and committed to differentiate.

However, the definitive underlying molecular mechanism that links low traction and low stiffness on soft substrates with undifferentiated growth of ESCs is not known at this time. One may hypothesize that the soft substrate may offer easy accessibility to LIF or other soluble growth factors produced

by ESCs themselves which in turn keep them in a sustained self-renewal state. Nevertheless, this hypothesis cannot explain how saturating amount of LIF and other soluble factors cannot keep ESC population on rigid substrate from differentiating. Therefore it is most probable that genes essential to sustain undifferentiated growth of ESCs are kept turned on by soft substrates via generation of low tractions. Future exploration using Microarray and gene expression profiling may unveil gene regulation mechanism by soft substrates.

Mechanical forces controls cell fate decisions of ESCs. The next relevant question arises which specific germ-layer they go to. This is left for future exploration. Additionally, the principle of matching substrate stiffness to intrinsic cell stiffness is likely to work for other cell types like human embryonic stem cells (hESCs). Currently, hESCs are cultured on Matrigel derived from EHS sarcoma. Identifying stiffness and functionalizing synthetic substrates for hESC culture would enable researchers a cheap, affordable, and xeno-free substrate. A recent report elegantly shows the importance of E-cadherin and nonmuscle myosin IIA (NMMIIA) in hESC self-renewal and pluripotency [6]. The optimized stiffness of the substrate should not, therefore, interfere with E-cadherin and NMMIA activities that could potentially affect long-term cell survival. Until recently, there has not been any standardized platform to test pluripotency of hESCs. One can easily make use of PluriTest [7] (an open-access bioinformatic assay of pluripotency in hESCs) to investigage hESC self-renewal and pluripotency status when cultured on an optimized substrate stiffness.

4.2 References

[1] del Rio, A. et al., "Stretching single talin rod molecules activates vinculin binding". *Science* 323, pp.638-641, 2009.

[2] Johnson, C.P., H. Y. Tang, C. Carag, D. W. Speicher, and D.E. Discher, "Forced unfolding of proteins within cells". *Science* 317, pp.663-666, 2007.

[3] Na, S. et al., "Rapid signal transduction in living cells is a unique feature of mechanotransduction". *Proc. Natl. Acad. Sci. U.S.A.* 105, pp.6626-6631, 2008.

[4] Holle, A.W. and A.J. Engler, "Cell rheology: Stressed-out stem cells". *Nature Materials* 9(1), pp.4-6, 2010.

[5] Gilbert, P.M. et al., "Substrate elasticity regulates skeletal muscle stem cell self-renewal in culture". *Science* 329(5995), pp.10781081, 2010.

[6] Li, D. et al., "Integrated biochemical and mechanical signals regulate multifaceted human embryonic stem cell functions". *Journal of Cell Biology* 191, pp.63144, 2010.

[7] Müller, F.J. et al., "A bioinformatic assay for pluripotency in human cells". *Nature Methods* 8(4), 315-317, 2011.

Figure 4.1: Mechanically induced differentiation

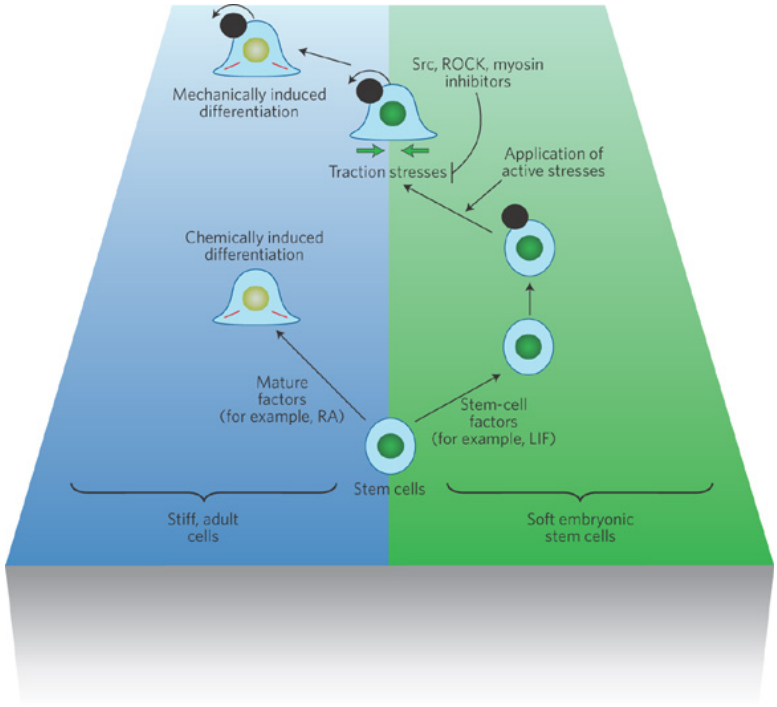

With chemical induced differentiation ESCs start to differentiate in response to small soluble molecules (left, gradient blue box) while mechanical induced differentiation (right, gradient green box) causes ESCs to spread and experience increased traction stresses. This stress leads to the downregulation of pluripotency gene OCT3/4 comparable to cells that had undergone chemical induced differentiation.[Holle, A. W. & Engler, A. J. (2010) Nature Materials 9(1), 4-6]

APPENDIX A

POLYACRYLAMIDE GEL RECIPE

A.1 Preparation and activating glass bottom dishes

Day 1:

Materials

1. 0.1N NaOH (Sigma-Aldrich, Product # S8045)

Method

1. Apply 1 drop (200 μl) of 0.1N NaOH on each glass bottom dishes
2. Let it air dry overnight

Day 2:

Materials

1. 3-aminopropyltrimethoxysilane (Aldrich, Product # 281778-100ml)
2. 0.5% gluteraldehyde (Sigma-Aldrich, Product # G6257)
3. Distilled Water (Milli-Q water)

Method

1. Smear 3-aminopropyltrimethoxysilane over the surface using a cotton-tipped swab and let it sit there for 6 min
2. Wash 2x with water for 15 min in shaker
3. Apply 100 μl/ dish of 0.5% gluteraldehyde and wait for 30 min
4. Wash with water for 15 min in shaker two times
5. Let them dry off
6. Activated dishes may be stored either in covered Petri dishes at room temperature for up to 48 hr or in a dessicator for two weeks

A.2 Polyacrylamide substrates

Day 3:

Materials

1. 40% Acrylamide (Bio-Rad, Product # 161-0140)
2. 2% Bis (Bio-Rad, Product # 161-0142)
3. Fluorescent latex beads (Fluospheres) if used (Molecular Probes, Red: 580/605, Yellow: 505/515)
4. Ammonium persulfate (Bio-Rad, Product # 161-0700) solution (APS)10% (w/v), mix with water
5. TEMED (Bio-Rad, Product # 161-0801)
6. 100 mM HEPES (Sigma, Product # H0887)

Method

1. Determine acrylamide: Bis solution proportions to get desired substrate stiffness [1]
2. Mix acrylamide: Bis solution of desired proportions w/o introducing bubbles
3. Degas the solution for 20 minutes to remove dissolved oxygen which inhibits acrylamide polymerization.
4. Sonicate beads for 1-3 min
5. Add of Activator/ Initiator of polymerization
   10% APS @ 1: 200 volume ratio
   TEMED @ 1: 2000 volume ratio.
6. Aliquot (10 μl would give $\sim$70 μm thick substrates and 15 μl would give $\sim$75 μm thick substrates) mixture on edge of activated glass bottom dishes
7. Flatten droplet w/ circular cover glasses (Fisher, Product # 12-545-80)

[1] Engler, A. et al., BioPhys. J. 2004; Yeung, T. et al., Cell Motil. Cytoskeleton, 2005

8. Turn the glass bottom dishes upside down. This ensures the beads to be closer to the top surface.
9. Wait for 30 min
10. Flood the surface w/ 2 ml 100 mM HEPES; it should not get dried
11. Carefully remove circular cover glasses with a single edge razor
12. Rinse the substrate well w/ 100 mM HEPES
13. The substrate may be stored w/ 100 mM HEPES at 4°C for two weeks

A.3 Activating substrates

Day 4:
Caution: This step is to be done in the dark. SANPAH is light and moisture sensitive

Materials

1. Crosslinker: Sulfo-SANPAH (Pierce, Product # 22589)
2. DMSO (Sigma, Product # D2650)
3. 100 mM HEPES (Sigma, Product # H0887)
4. Col I (0.1 mg/ ml)

Method

1. Make 1mM solution of SANPAH in 100 mM HEPES.
2. Take out HEPES from the glass bottom dishes, dab excess HEPES with Kim wipes from around gel edge
3. Apply 200 μl of freshly made SANPAH solution on each dish
4. Expose surface under 302 nm UV for 6 min (no more than 6 inch away from the lamp). SANPAH will darken when used up
5. Rinse off SANPAH w/ HEPES in the shaker
6. Repeat photo activation procedure

7. Wash 1x for 3-4 min in 100 mM HEPES **w/o** shaking
8. Cover substrates w/ Col I (0.1 mg/ ml)
9. Incubate overnight at 4°C
10. Wash gently w/ PBS
11. Sterilize under UV light for 20 min
12. Substrates can be stored at 4°C in PBS for two weeks

A.4 Plating cells on substrates

Day 5:

Method

1. Soak gels for 30-45 min in culture medium in an incubator
2. Plate cells at desired density: 3000- 5000 cells/ dish. Cells would normally be ready by overnight

AUTHOR'S BIOGRAPHY

Farhan Chowdhury received his Bachelor of Science degree (with Honors) in Mechanical Engineering from Bangladesh University of Engineering and Technology (BUET) in 2003. For next one and a half years Chowdhury worked as a Lecturer in the Department of Mechanical Engineering at the same university before starting his graduate studies at Tuskegee University. He finished his Master of Science degree in Mechanical Engineering from Tuskegee University in 2006. Then he decided to join University of Illinois to pursue PhD in Mechanical Engineering from Fall 2006. His research focuses on understanding cell fate decisions of embryonic stem cells by physical and mechanical cues. Following the completion of his PhD, Chowdhury will begin to work as a Post Doctorate Research Associate in the Department of Mechanical Science and Engineering at the University of Illinois at Urbana-Champaign.